Pak. J. Bot., 58(1): 147-163, January 2026.

ARTICLE | DOI: http://dx.doi.org/10.30848/PJB2026-1(14)

MICROSTRUCTURAL AND FUNCTIONAL TRAITS FACILITATE INVASION OF HONEY MESQUITE (*NELTUMA GLANDULOSA* (TORR.) BRITTON & ROSE) IN ENVIRONMENTAL HETEROGENEITY

ZOYA NAZISH[1], FAROOQ AHMAD[1], MANSOOR HAMEED[1] AND MUHAMMAD ASHFAQ WAHID[2]

[1]Department of Botany, University of Agriculture Faisalabad, Faisalabad 38040, Pakistan
[2]Department of Agronomy, University of Agriculture Faisalabad, Faisalabad 38040, Pakistan

*Corresponding author's email: hameedmansoor@yahoo.com

Abstract

Species diversity in any ecosystem depends on the environmental heterogeneity. Plants respond to stresses in a heterogeneous environment through various structural and functional modifications for their establishment and invasiveness. Honey mesquite (*Neltuma glandulosa* (Torr.) Britton & Rose) is an invasive weed found in all types of habitats ranging from high mountains to deserts and its invasion success might be due to plasticity in structural and functional traits. Its populations were collected from eight geographically distinct sites of Punjab to evaluate structural and functional modifications in diverse environmental conditions. Significant variation was found in morphological traits, chlorophyll pigments, stress enzymes, organic osmolytes, antioxidants, ionic content, foliar and stem anatomical traits that show high adaptability potential of this species to different habitats. Populations collected from non-saline habitats showed better growth and development. Highest concentration of organic osmolytes, stress enzymes, antioxidants and vitamins was in population from hypersaline saltmarsh. Regarding anatomical traits thick epidermis and large parenchymatous cells were found in the sand dune desert population, a better strategy to protect water loss and to store sufficient amount of water in the stem. Stem sclerification was high in the hypersaline hyperarid population to tolerate environmental stresses. Hypersaline hyper-arid population had maximum stomatal density and decreased stomatal area that assist in lowering transpiration loss. The findings indicated that invasion and widespread of this species was due to plasticity in structural and functional traits. Physio-anatomical tools can play a key role in evaluating adaptive components, hence can be extremely useful to understanding mechanism of invasion in plant specues.

Key words: Honey mesquite**,** Organic osmolytes, Stress enzymes, Sclerenchyma, Parenchyma, Invasion.

Introduction

Environmental heterogeneity plays a crucial role to determine species diversity in an ecological community. Habitat heterogeneity or variations in environmental conditions depicts fundamental ecological processes within an ecosystem, such as competition and resource allocation. This variability enables diverse species to adapt by accessing differential resource opportunities, thereby enhancing species diversity (Moore & Schindler, 2022). The Punjab province in Pakistan is characterized by distinctive ecosystems that developed under influence of unique environmental factors, landscape and other natural factors endorsing ecological stability (Akhter *et al*., 2021). Thus, the area is naturally divided into various ecoregions exhibiting significant differences in micro- and macro-habitat due to multiple stresses such as drought, temperature and salinity. Consequently, these ecosystems create a mosaic of habitats each with its own unique set of environmental conditions such as soil, temperature, availability of water as well as exposure to multiple stresses. Habitat heterogeneity in Punjab not only bolsters ecological resilience but also nurture species diversity as in such heterogeneous environment species thrive to adapt the specific or challenging environment (Falk *et al*., 2022). These variable conditions provide excellent opportunities for invasive species proliferation, as they adapt to heterogeneous or challenging environment (Mengistu *et al*., 2023).

Environmental stresses such as salinity, drought, and temperature are major hindrances to growth and developmental of a plant species. Consequently, in a heterogeneous environment, the combination of these abiotic stresses shapes major patterns of a plant species in an ecosystem. Plants may respond to abiotic stresses in a heterogeneous environment via structural and functional variability. These are adaptive responses to promote average fitness of a species. The variations in structural and functional traits aim to promote adaptations to harsh environmental conditions across the environmental gradient (Pazzagila *et al*., 2021). Funk *et al*., (2020) declared physiological and morphological trait modifications as an adaptive response to environmental heterogeneity, directly related to population fitness. The morpho-anatomical and physiological modifications are those structural and functional attributes which lead to the ultimate establishment of invasive species (Avanesyan, 2021).

The negative impact of invasive species is well documented (Divisek *et al*., 2018; Dawkins *et al*., 2022). They elicit irreversible structural and functional modifications in an ecosystem. Hui & Richardson, 2017, including loss of biodiversity, soil physico-chemical characteristics, which potentially reduce or enhance ecosystem productivity (Kull, 2018). The invasive species tend to be more resilient than native species (Sharma *et al*., 2022). Once established, invasive species grow at an exponential rate because of their ability to cope with environmental stresses in a complex manner (Owasa *et al*., 2020), inevitably driving spatial and biophysical patterns of ecosystems in arrival areas and expanding their distribution range (Sharma *et al*., 2022). As

Received: 10-03-2025 | Revised: 30-04-2025 | Accepted: 02-05-2025 | Online: 02-09-2025

confirmed by Shackleton *et al*., (2019) in various canopy base analyses, all spatial components of native species in an ecological community, i.e., canopy cover, basal cover, richness, basal area, density, and all other spatial component become affected by alien species. Some key drivers of species invasion in natural ecosystem are disturbance, lack of natural enemies, better resource allocation, lack of abiotic and biotic stresses and differential reproductive abilities (Ibanez *et al*., 2021). Various physiological and morphological adaptations particularly assist successful establishment of invasive species (Avanesyan, 2022).

Because of their great seed output, fire resistance, and better competitive powers, certain *Neltuma* species can quickly take over freshly colonized regions (van Wilgen *et al*., 2024). In areas where *Neltuma* species have established, allelopathy has been proposed as one of the processes that enable them to gain dominance (Bibi *et al*., 2023). *Neltuma* species have morphological and physiological adaptations that enable them to avoid or tolerate the environmental constraints, enabling them to grow, live, and procreate in saline, dry, and semi-arid habitats (Gul *et al*., 2022). *Neltuma* species is a phytoremediator that can greatly lower the salinity level of soil and withstand both arid and salty environments (Kumar *et al*., 2021).

Neltuma glandulosa (Torr.) Britton & Rose (previously known as *Prosopis glandulosa*) is an invasive weed with a global reputation for its detrimental impact on soil, human and animals, and ecosystems (Shackleton *et al*., 2015). It occurs almost in all provinces of Pakistan. Initially it was introduced for sand dunes stabilization and timber production but it is now wide spread in Khyber Pakhtoonkhwa (Pabbi hills), Punjab (Potohar Plateau) and Sindh (Makran). In Balochistan *Neltuma* has invaded all natural and artificial ecosystems, from flat plains to Rocky Mountains, from saline soil and coastal areas, disrupting natural vegetation (Tabassum *et al*., 2015). It is established in plain and waterlogged areas, desert, riparian range land and highways (Rashid *et al*., 2014). This tree can grow at an exponential rate in a rangeland (Belnap *et al*., 2012). Hence, all areas of Pakistan are suitable for its growth.

As is true for the leguminous tree, *N. glandulosa* is capable of enriching the soil via symbiosis, which enables it to withstand the harsh arid environment (Shackleton *et al*., 2014). Moreover, it can tolerate high soil alkalinity (9.5 to 10.0 pH) (Chaturvedi *et al*., 2016). The root can actually grow up to 50 meters deep. *N. glandulosa* has extensive surface root system in addition to deep root system; hence, *N. glandulosa* put on fierce competition on other plant species for acquisition of soil mineral and nutrients in an ecosystem due to its extensive root system (Ellsworth *et al*., 2018). *Neltuma* can grow up to 7.6 meters. Moreover, it had ability to quickly retrieve growth after drought. Eradication efforts stimulate growth aggression in *N. glandulosa* (Abbas *et al*., 2019). Research has declared ability of young tree to grow on least fertile soil and tolerance against high salinity (Le Houérou *et al*., 2012). They can reabsorb nitrogen and phosphorous from the litter (Soper *et al*., 2015).

Micromorphological features of invasive species like *N. glandulosa* are understudied, especially in response to environmental heterogeneity. Linking plasticity in structural and micromorphological traits is critical for evaluating adaptability potential in widespread and invasive species. No literature has been reported earlier to in *N. glandulosa* to assess ecological success modulated by plasticity in structural and functional traits. In the present we will focus on the following research questions: a) Is there any variation in structural and functional of *N. glandulosa* traits growing in a variety of habitats? b) If yes, then how plasticity in these traits contributes in invasion success of *N. glandulosa*? and c) how soil and environmental factors correlates with structural and functional traits? We expect that plasticity in structural and functional traits can play a critical role in invasion success and adaptability potential in ecologically different habitats.

Methodology

Collection sites and sampling procedure: Different ecoregions of Punjab were explored for the collection *N. glandulosa,* which was established in almost all ecoregions of Punjab from lower desert plains to lush green mountainous region. For collection of plant material, eight geographically distinct sites with differentially adapted populations were selected (Fig. 1). The selection of collection sites was systematic based on a great variation in soil structure and physiological traits, topography, environmental traits and physiographic traits. Samples from *N. glandulosa* populations in arid region were collected from low sand dunes (Nawab Shah), hypersaline desert plain (Ladam Sar) and from coarse sand desert (Sakhi Sarwar). Samples were also collected from highest peak in Suleman Range (Fort Munro). Samples from semiarid region populations growing in saline areas were collected from salt affected dry land salt mine (Warcha Saltmine) and surrounding area of hypersaline saltmarsh (Khabbeki). Samples were also collected from deep valley surrounded by dry mountains (Neela Wahn) and near mountain spring in mountains valley (Dape Sharif). Five plants of average size growing at an average distance of at least 10 meters were randomly selected and considered as replications. The plant material was carefully collected and sealed in a zipper and was kept in icebox and later brought to laboratory for further analysis. The populations of *N. glandulosa* were evaluated for structural and functional modifications in diverse environmental conditions.

Geographic and environmental data: Geographic aspects, i.e., elevation, longitude and latitude were recorded. The Coordinates and elevation data was recorded by Global Positioning System (Garmin eTrex Venture HC, USA). The aspect of collection sites was measured by magnetic compass (Pocket Geological Plastic Compass, USA). The slope value was measured by Digital inclinometer 27 (LD360 Electronic inclinometer, USA). Meteorological data of collection sites including annual rainfall, maximum and minimum annual temperature were collected from regional observatories of PMD (Punjab Meteorological Department).

Soil analysis: The soil of near each selected plant of each population was collected for soil physiochemical analysis at about 16 cm depth. Soil was persevered in polythene bag after precise labeling. A 200 g of oven dried soil at about 70°C was used to determine soil saturation percentage. Soil ECe, pH and soil organic matter was measured by pH/Electrical Conductivity Meter (WTW series InoLab pH/Cond 720, United Kingdom). Soil Na^+, K^+, and Ca^{2+} were measured using flame photometry (Jenway, PFP-7, Dunmow Essex, UK) by running a series of samples (10-100 mg L^{-1}) and standard curves following the methods described in Handbook No. 60 (Richards, 1954).

The following formulas were used to estimate soil saturation percentage and soil organic matter

$$\text{Saturation percentage} = \frac{\text{Weight of water required to saturate the soil}}{\text{Weight of the dry soil}} \times 100$$

$$\text{Organic matter \% age} = \frac{S - T}{S} \times 6.7$$

where, S= blank reading; T= Volume used of $FeSO_4$

Anatomical attributes: Fresh plant material was collected and immediately transferred to concealed bottles containing formaline acetic alcohol (FAA) with v/v ratio given below:

FAA = Formalin (5%) + Acetic acid (10%) + Ethanol (50%) + Distilled water (35%)

After 48 hours the plants material was transferred in acetic alcohol solution with following v/v ratio:

Acetic alcohol = Acetic acid (25%) + Ethanol (75%)

Permanent slides were made using free-hand sectioning technique. A series of ethanol grades (30%, 50%, 70%, 90% and the absolute 100 %.) was used to dehydrate plant transverse sections. Two dyes fast green and safranin were used to stain lignified and parenchymatous tissues respectively. The prepared transverse sections were treated with xylene and were affixed on glass slide by DPX and were covered with coverslips. Camera equipped digital compound microscope (Meiji Techno, Japan) was used to capture digital photographs. Microstructural data of transverse sections was measured by ocular micrometer. Stem and leaf anatomical characters were evaluated. The micrographs were taken on 40X magnification.

Physiological attributes: Ionic content was determined according to Wolf (1982) outlined methodology. Dried 0.1 g plant material was digested in concentrated H_2SO_4 and Na^+, K^+ and Ca^{2+} concentrations were estimated through flame photometer (Jenway, PFP-7, UK).

Methodology outlined by Arnon (1949) was used for estimation of photosynthetic pigments. For this purpose, 0.1 g of leaves was grounded and soaked overnight in 5ml 80% acetone. Optical density (OD) records were made on spectrophotometer (Hitachi 220, Japan) at 480, 645 and 663nm while keeping 80% acetone as blank. Following formulas were used to calculate pigment content:

$$\textit{Chl. a } (mgg^{-1} \textit{ f. wt.}) = [12.7\,(OD663) - 2.69(OD645)] \frac{V}{1000} \times W]$$

$$\textit{Chl. b } (mgg^{-1} \textit{ f. wt.}) = [22.9\,(OD645) - 4.68(OD663)] \frac{V}{1000} \times W]$$

$$\text{Total } (mgg^{-1} \textit{ f. wt.}) = [20.2\,(OD645) - 8.02(OD663)] \frac{V}{1000} \times W]$$

Carotenoids (mgg^{-1} f.wt.) = [12.7 (OD480) – 0.114 (OD663)] – 0.638 (OD645)]/2500

where V = Volume of the sample, W = Weight of fresh tissue

The protocol outlined by Bradford (1976) was followed in order to evaluate total soluble proteins of supernatant. For this purpose 0.25 g leaves grinding in 10 ml of potassium phosphate buffer solution of 50 mM molarity was followed by centrifugation, then OD of mixture comprising 5 µl of sample, 95 µl of 1N NaCL and 1ml Bradford dye, was taken on spectrophotometer (Hitachi 220, Japan) at 595 nm.

Velikova *et al*., (2000) protocol was followed to estimate H_2O_2 concentration. For this purpose in an icy mortar 0.25 g leaves were grounded in 5 ml of 0.1% trichloroacetic acid and subsequently centrifuged, then solution mixture of 0.5 ml of supernatant, 0.5 ml 50 mM potassium phosphate buffer and 1 ml of 1M KI was vortexed and OD was measured on spectrophotometer (Hitachi 220, Japan) at 390nm while keeping distilled water as blank.

A Thiobarbituric Acid Reactive Substances/TBA-based assay by Carmak & Horst (1991) was used for estimation of malondialdehyde (MDA). Leaf extract of 0.25 g in 5 ml 1% (w/v) TCA was centrifuged, and then supernatant was kept in water-bath for about 1 h after mixing with 20% TCA and was again centrifuged for 10 min. The Malondialdehyde of mixture reacted with thiobarbituric acid forming a detectable pink chromogen TBARS. Absorbance was recorded on spectrophotometer (Hitachi 220, Japan) at 532 and 600 nm and TBARS level was calculated using coefficient E_o

$$\text{Melondialdehyde } (\mu mol\ l^{-1}) = \frac{\text{Absorbance of a sample}}{E_o \times L} \times D$$

where E_o = Extinction coefficient 1.56 x 10^5 M^{-1} cm^{-1}, L = Light path cm, D = Dilution factor 6.7 x 10^6

To analyze antioxidant enzyme activities, a leaf extract of 0.25 g leaves was prepared in 50 mM of 5 ml KP buffer while ensuring mortar ice cold. Following the subsequent centrifugation at 4°C for 15 minutes, the supernatant was removed and was further used for determination of antioxidant enzymes.

To evaluate superoxide dismutase (SOD) activity, the enzyme assay outlined by Giannopolitis & Ries (1977) was followed. As per instructions, in the following order a reaction mixture was prepared and placed under lamp for 15 min.: 250 µl KP buffer + 400 µl distilled water + 100 µl L-methionine + 100 µl triton+ 50 µl NBT + 50 µl riboflavin + 50 µl supernatant.

To estimate catalase (CAT) activity, enzyme assay developed by Chance & Maehly (1955) was followed. The absorbance of reaction mixture in following order was record at 240 nm at regular intervals of 30 seconds for a minute: 1.9 ml 50 mM KP buffer + 100 µl H_2O_2 + 100 µl.

The Peroxidase (POD) activity was assayed after methodology developed by Chance & Maehly (1955). The OD of reaction mixture in following order was measured at 470 nm at regular intervals of 30 second for a minute: 750 µl of 50 mM KP buffer, 100 µl of guaiacol, 100 µl of H_2O_2 and 50 µl of the sample.

To estimate leaf proline content 0.1 g of leaf was taken and triturated against 2 ml 3% sulphosalicylic acid. For trituration protocol outlined by Bates *et al*., (1973) was followed. Following trituration sample was ultra-centrifuged for 10 minutes and then filtered. Next, a mixture in following proportions was prepared to be heated in water-bath for an hour: 1ml filtrate + 1 ml acid ninhydrin + 1 ml glacial acetic acid. After water-bath treatment, the mixture was chilled and

5 ml toluene was added. Then, the mixture was vortexed resulting in separations of two layers within reaction mixture. OD of upper layer was taken at 520 nm. Total Proline content was calculated by following formula:

$$\text{Proline } (\mu\text{mol g}^{-1} \text{ fresh weight}) = \frac{\mu\text{g proline } (\text{ml}^{-1}) \text{ x ml of toluene}}{15.5 \text{ sample weight (g)}}$$

To evaluate total phenolics Julkenen-Titto (1985) methodology was used. Leaf extract of 0.1 g leaves was prepared 1ml of 80% acetone and centrifuged. Mixture was vortexted in two intervals. Firstly 100 µl supernatant + 1ml DW + 0.5ml Folin Phenol reagent were added and mixture was vortexed. Then, 2.5 ml 20% Na_2CO_3 was added and mixture was vortexed again for 5 seconds. OD was taken at 750 nm while keeping 80% acetone as blank after 20 minutes.

The ascorbic acid content was determined by methodology outlined by Mukerjee & Choudhri (1983). Leaves (0.1 g) were ground in 5 ml of 6% TCA and centrifuged. A mixture containing 1 ml aliquant and 2% DNPH was prepared in 9 N H_2SO_4 containing a drop of 10% ethanol thiourea. Then, the mixture was heated in a water-bath. After 15 minutes the mixture was cooled at 0°C and 1.5 ml of 80% v/v H_2SO_4 was added. OD was measured at 530 nm.

Statistical analysis

One way ANOVA in completely randomized design with five replications was run to test significant variation. Duncan's Multiple Range test was applied for comparison of means. The association among different variable was checked by Principal Component Analysis (PCA) using XLSTAT (ver. 2014). The first and second principal components, or PC1 (F1) and PC2 (F2), respectively, capture the greatest and second-most variation in a dataset.

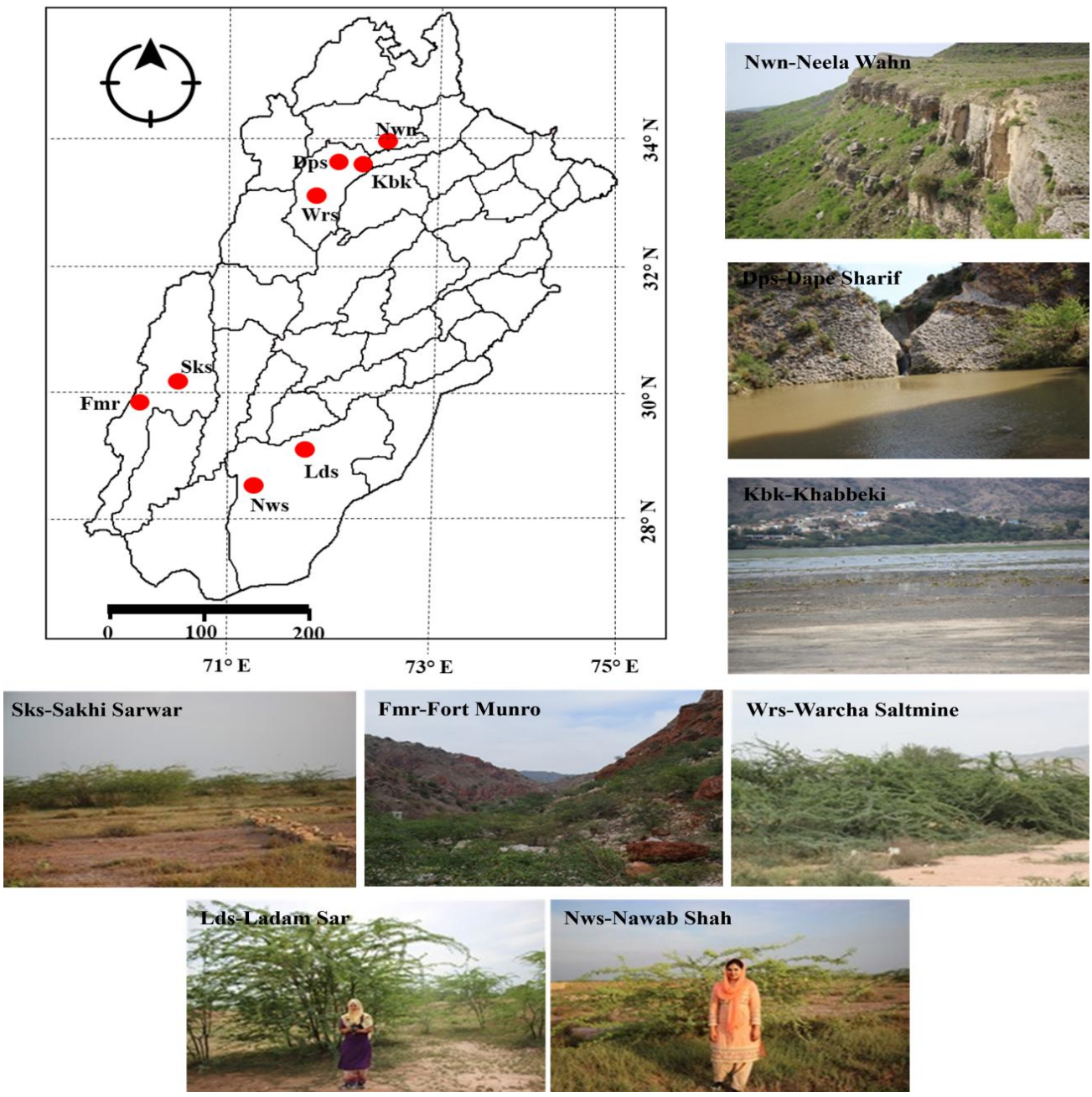

Fig. 1. Map of the Punjab showing collection sites of *Neltuma glandulosa* and pictorial view of habitats.

Table 1. Environmental and soil physicochemical characteristics and metrological record of Neltuma glandulosa collection sites in the diverse ecozones.

	Nawab Shah	Ladam Sar	Neela Wahn	Sakhi Sarwar	Fort Munro	Warcha Saltmine	Khabbeki	Dape Sharif
Environmental traits								
Elevation (m a.s.l.)	98g	140f	538d	267e	1839a	288e	813c	1012b
Average maximum temperature (°C)	45a	41b	33d	41b	32d	34c	44a	35c
Average minimum temperature (°C)	10a	8b	3d	6c	−1e	11a	9b	4d
Annual rainfall (mm)	120e	200d	658a	155e	246d	400c	600b	459c
Soil physicochemical traits								
pH	8.4 ± 0.65a	6.4 ± 0.45e	8.1 ± 0.73b	7.3 ± 0.44d	7.5 ± 0.59d	6.8 ± 0.47e	7.5 ± 0.58d	7.7 ± 0.55c
ECe (dS m−1)	1.3 ± 0.39e	40.2 ± 2.33b	2.7 ± 0.42d	1.1d ± 0.16e	2.6 ± 0.13d	22.4 ± 1.03c	47.0 ± 3.39a	2.3 ± 0.13d
Ca2+ (mg kg−1)	78.8 ± 3.29d	62.4 ± 2.47e	105.5 ± 9.3c	188.0 ± 13.4a	127.4 ± 10.27b	84.5 ± 3.25d	115.4 ± 8.8c	124.4 ± 10.13b
K+ (mg kg−1)	115.4 ± 9.8d	68.4 ± 4.29e	179.4 ± 13.62b	48.8 ± 2.67f	167.4 ± 13.44c	155.5 ± 11.18d	166.3 ± 9.9c	350.5 ± 17.12a
Na+ (mg kg−1)	64.1 ± 1.89e	4644.1 ± 132.6b	81.4. ± 2.4d	65.7 ± 1.12e	84.9 ± 1.99d	3443.3 ± 125.7c	5135.2 ± 136.2a	82.6 ± 2.1d
NO3− (mg kg−1)	8.7 ± 0.65b	3.2d ± 0.14d	3.7 ± 0.45c	13.4 ± 4.56a	3.1e ± 0.26	3.2 ± 0.24d	3.4 ± 0.33d	3.6 ± 0.28c
PO43− (mg kg−1)	3.1 ± 0.17f	6.8 ± 0.41d	4.0 ± 0.36e	8.4 ± 0.43c	14.0 ± 0.99a	10.9 ± 0.78b	4.3 ± 0.40e	6.1 ± 0.55d
Organic matter (%)	0.62 ± 0.03f	0.83 ± 0.05d	0.62 ± 0.03f	0.99 ± 0.01c	1.60a ± 0.13a	1.04 ± 0.08b	0.83 ± 0.02d	0.76 ± 0.03e
Saturation percentage (%)	13.0 ± 1.33f	19 ± 1.51e	24.0 ± 1.04d	28.0 ± 0.09b	31.0 ± 1.21a	26.0 ± 1.18c	24.0 ± 1.25d	25.0 ± 1.71c

Results

Environmental and soil physicochemical traits: The average maximum temperature of arid desert areas ranged between 45-41°C whereas the minimum temperature was between 6-10°C (Table 1). The maximum temperature was 32°C in arid mountain Fort Munro-the highest peak of Suleiman range whereas the minimum temperature at Fort Munro was –1°C. The maximum temperature of saline areas was Khabbeki, Warcha Saltmine and Ladam Sar was 44°C, 34°C and 41°C respectively whereas the minimum temperature was 9°C, 11°C and 8°C respectively. The maximum temperature was 35°C and 33°C in deep valley Neela Wahn and at mountain spring areas Dape Sharif respectively whereas the minimum temperature was 3°C and 4°C respectively. Annual precipitation was relatively high in deep valley Dape Sharif and at hypersaline salt marsh Khabbeki while in desert area annual precipitation was as low as 155 mm or even below 125 mm.

Soil pH ranged from 6-8 at all sites (Table 1). Soil ECe was quite high in hypersaline areas Khabbeki and Ladam Sar, which was ECe > 40 dS m^{-1}. The soil ECe was 22.4 dS m^{-1} at Warcha Saltmine while it ranged between 1-3 dS m^{-1} at all other sites. Soil Na^+ was the highest in saline areas. Soil Ca^{2+}, NO_3^- was the highest in coarse sand desert, whereas K^+ was the highest at mountain spring Dape Sharif. Soil PO_4^{3-} was the highest at Fort Munro. Organic matter was the highest at mountain peak Fort Munro and it was lowest in deep valley Neela Wahn. Soil saturation percentage was the highest at mountain peak Fort Munro while it ranged between 24-28% at all other sites with exception of hypersaline desert plain Ladam Sar and low sand dunes Nawab Shah where it was 19% and 13% respectively.

Morphological traits: The nonsaline areas (Nawab Shah and Dape Sharif) supported optimum growth of *Neltuma* with tall plants having higher biomass allocation and large leaves, whereas the saline areas (Ladam Sar, Warcha Saltmine and Khabbeki), extreme environment of desert areas (Sakhi Sarwar and Nawab Shah) and mountain peak (Fort Munro) exhibited moderate growth of *Neltuma* populations (Table 2). Saline habitats and nonsaline habitat (Dape Sharif) tend to have higher number of branches with higher leaf densities and higher leaf area per branch in nonsaline area Dape Sharif.

Population of deep valley (Neela Wahn) showed the maximum plant height (5.9 m) and the maximum shoot fresh and dry weights (66.4 g $plant^{-1}$, 11.0 g $plant^{-1}$, respectively). Leaf area was also high (4518.4 cm^2) in Neela Wahn population (Table 2). Population of mountain spring (Dape Sharif) exhibited moderate height (3.9 m) but the maximum leaf area (4608 cm^2) with relatively high biomass allocation and moderate leaf density. Large leaves were observed in populations at both these sites; however leaf density was the minimum at Neela Wahn (15).

Table 2. Morphological and physiological characteristics of Neltuma glandulosa populations collected from diverse ecozones.

	Nawab Shah	Ladam Sar	Neela Wahn	Sakhi Sarwar	Fort Munro	Warcha Saltmine	Khabbeki	Dape Sharif
Morphological characteristics								
Number of branches	8.3 ± 0.69e	10.7 ± 0.99c	8.7 ± 0.77d	9.7 ± 0.72c	8.7 ± 0.54d	14.3 ± 1.93a	14.3 ± 1.87a	12.0 ± 1.01b
Plant height (m)	1.7 ± 0.14e	4.2 ± 0.17c	5.9 ± 0.34a	4.7 ± 0.35b	3.9 ± 0.49d	4.4 ± 0.52c	3.7 ± 0.59d	3.9 ± 0.24d
Number of leaves per branch	18.0 ± 1.17d	32.0 ± 1.24b	15.0 ± 1.19e	21.0 ± 1.31c	21.0 ± 1.04c	31.0 ± 1.21b	51.0 ± 2.31a	22.0 ± 1.44c
Leaf area per branch (cm2)	26.0 ± 1.32f	80.0 ± 4.24e	4518.4 ± 121.1b	215.0 ± 14.32d	191.0 ± 13.19d	57.6 ± 2.45e	1242.0 ± 105.3c	4608.0 ± 167.2a
Shoot fresh weight (g plant-1)	10.8 ± 1.03e	9.0 ± 0.79f	66.4 ± 3.48a	33.6 ± 1.41c	33.8 ± 1.29c	59.0 ± 2.99b	28.8 ± 1.33d	58.6 ± 3.16b
Shoot dry weight (g plant-1)	1.8.0 ± 0.17e	1.5 ± 0.16e	11.0 ± 0.89a	5.6 ± 0.14c	5.6 ± 0.19c	9.8 ± 1.0b	4.8 ± 0.26d	9.8 ± 0.83b
Chlorophyll pigments								
Chlorophyll a (mg g^{-1} f.w.)	1.7 ± 0.13d	1.6 ± 0.15e	2.0 ± 0.19b	1.9 ± 0.18c	2.0 ± 0.17b	1.8 ± 0.12d	1.5 ± 0.14f	2.1 ± 0.18a
Chlorophyll b (mg g^{-1} f.w.)	0.6 ± 0.015e	0.7 ± 0.014d	1.0 ± 0.019b	0.9 ± 0.013c	1.0 ± 0.018b	0.8 ± 0.014d	0.5 ± 0.006f	1.1 ± 0.029a
Total chlorophyll (mg g^{-1} f.w.)	2.3 ± 0.33e	2.3 ± 0.12e	2.9 ± 0.19b	2.8 ± 0.21c	3.0 ± 0.18b	2.6 ± 0.19d	2.0 ± 0.14f	3.2 ± 0.26a
Chlorophyll a/b (mg g^{-1} f.w.)	2.8 ± 0.21b	2.4 ± 0.29c	2.0 ± 0.13e	3.2 ± 0.21a	2.1 ± 0.37e	2.3 ± 0.19d	2.0 ± 0.11e	1.9 ± 0.19f
Carotenoids (mg g^{-1} f.w.)	0.061 ± 0.03c	0.082 ± 0.02a	0.084 ± 0.06a	0.065 ± 0.04c	0.087 ± 0.03a	0.072 ± 0.04b	0.084 ± 0.05a	0.086 ± 0.02a
Stress enzymes								
Catalase (U mg–1 protein)	4.5 ± 0.23c	5.5 ± 0.27a	2.2 ± 0.19f	3.7 ± 0.14d	3.6 ± 0.58d	4.8 ± 0.26c	5.4 ± 0.32b	2.5 ± 0.10e
Superoxide dismutase (U mg–1 protein)	0.72 ± 0.034b	0.81 ± 0.067a	0.13 ± 0.019e	0.65 ± 0.011c	0.47 ± 0.013d	0.72 ± 0.025b	0.86 ± 0.01 a	0.32 ± 0.025d
Peroxidase (U mg–1 protein)	5.0 ± 0.29d	7.1 ± 0.16a	4.9 ± 0.33d	4.4 ± 0.24e	3.6 ± 0.16f	5.6 ± 0.13c	6.8 ± 0.19b	3.2 ± 0.11f
Organic osmolytes								
Total soluble proteins (µg g^{-1} f.w.)	1061.0 ± 19b	1065.1 ± 11b	572.5 ± 12.7e	570.8 ± 11.1e	775.5 ± 21.1d	967.5 ± 0.17c	1570.5 ± 31.3a	520.5 ± 12.9f
Total soluble sugars (mg g^{-1} f.w.)	18.4 ± 0.04b	21.6 ± 0.05a	12.7 ± 0.02c	11.5 ± 0.02c	8.6 ± 0.03d	19.3 ± 0.02b	23.8 ± 0.01a	7.1 ± 0.03d
Total free amino acids (µg g–1 f.w.)	201.5 ± 13.3d	321.7 ± 31.3b	215.9 ± 14.1d	235.4 ± 17.1c	182.4 ± 12.5e	315.6 ± 32.1b	421.5 ± 36.2a	142.1 ± 11.1e
Proline (µmol g^{-1} f.w.)	88.1 ± 4.04d	123.4 ± 10.01a	94.7 ± 7.02c	108.2 ± 11.04b	109.7 ± 9.06b	101.1 ± 9.01b	127.7 ± 10.03a	82.1 ± 3.01d
Glycine betaine (µmol g^{-1} f.w.)	2.1 ± 0.11c	2.2 ± 0.09b	2.0 ± 0.14d	1.8 ± 0.1e	1.9 ± 0.14d	2.1 ± 0.14c	2.3 ± 0.11a	2.3 ± 0.15a
Antioxidants, ROS and vitamins								
Malondialdehyde (µmol g^{-1} f.w.)	2.0 ± 0.11c	2.4 ± 0.14a	1.9 ± 0.11d	1.0 ± 0.13f	1.2 ± 0.14e	2.0 ± 0.12c	2.2 ± 0.29b	1.4 ± 0.14e
Hydrogen peroxide (µmol g^{-1} f.w.)	38.2 ± 0.2c	42.5 ± 0.2b	30.7 ± 0.4d	29.2 ± 0.1e	33.5 ± 0.4d	42.6 ± 0.8b	50.3 ± 0.2a	31.6 ± 0.3d
Ascorbic acid (µg g^{-1} f.w.)	0.13 ± 0.07b	0.26 ± 0.08a	0.14 ± 0.01b	0.17 ± 0.03b	0.12 ± 0.07b	0.23 ± 0.01a	0.25 ± 0.06a	0.11 ± 0.03b
Phenolics (mg g^{-1} f.w.)	1.8 ± 0.19d	2.0 ± 0.11b	1.8 ± 0.12d	1.8 ± 0.15d	1.4 ± 0.11f	1.9 ± 0.12c	2.4 ± 0.17a	1.5 ± 0.1e
Ionic content								
Shoot K+ (mg g-1 d.w.)	3.3 ± 0.9f	8.5 ± 0.67c	6.7 ± 0.91d	5.3 ± 0.19e	8.8 ± 0.28c	9.6 ± 0.33b	11.5 ± 0.99a	5.5 ± 0.13e
Shoot Na+ (mg g-1 d.w.)	9.3 ± 1.88f	41.4 ± 1.28b	13.8 ± 1.34d	10.2 ± 1.26e	14.7 ± 1.33b	33.2 ± 1.26d	42.6 ± 1.33a	9.0 ± 1.29c
Shoot Ca2+ (mg g-1 d.w.)	21.5 ± 1.31c	33.4 ± 1.11a	23.1 ± 1.4b	18.9 ± 1.2d	8.6 ± 0.39e	8.2 ± 0.42e	23.7 ± 1.41b	21.3 ± 1.33c

Bold black fonts indicate the maximum value, while red bold fonts the minimum values

Table 3. Stem and leaf anatomical characteristics of Neltuma glandulosa populations collected from diverse ecozones.

	Nawab Shah	Ladam Sar	Neela Wahn	Sakhi Sarwar	Fort Munro	Warcha Saltmine	Khabbeki	Dape Sharif
Stem anatomical parameters								
Epidermal thickness (µm)	60.6 ± 3.43a	54.5 ± 2.56b	9.7 ± 0.67c	54.5 ± 3.33b	8.5 ± 0.54d	9.1 ± 0.44c	9.7 ± 0.55c	8.5 ± 0.68d
Sclerenchyma cell area (µm2)	3.9 ± 0.08g	354.5 ± 27.65a	233.5 ± 22.8b	5.2 ± 0.19f	77.8 ± 3.79d	145.3 ± 16.9c	145.3 ± 11.87c	51.9 ± 3.78e
Sclerenchyma thickness (µm)	127.2 ± 10.97b	133.2 ± 9.89a	84.8 ± 4.3c	54.5 ± 2.39e	78.7 ± 5.5c	66.6 ± 4.67d	60.6 ± 3.98d	109 ± 13.9b
Cortical thickness (µm)	218.2 ± 17.4b	145.4 ± 11.4c	77.5 ± 6.4d	54.5 ± 3.4e	151.4 ± 10.94c	90.9 ± 7.8d	139.3 ± 7.89c	254.4 ± 18.4a
Cortical cell area (µm2)	1297 ± 114.3a	518.8 ± 60.4c	778.2 ± 57.1b	64.9 ± 2.36e	311.3 ± 24.3d	5.2 ± 0.38e	145.3 ± 11.18d	778.2 ± 67.4b
Vascular bundle thickness (µm)	781.3 ± 56.8c	654.1 ± 55.7d	684.4 ± 59.7d	666.2 ± 59.7d	581.4 ± 33.86e	841.9 ± 66.9c	1066 ± 102.4a	957 ± 78.9b
Xylem thickness (µm)	666.2 ± 54.5c	575.4 ± 77.8d	648.1 ± 45.7c	648.1 ± 55.6c	563.3 ± 33.26e	823.7 ± 78.0b	999.4 ± 77.7a	902.4 ± 84.5b
Metaxylem area (µm2)	5706.9 ± 234.5b	4669.2 ± 356.7c	6485.1 ± 553.6a	454 ± 22.6f	1642.9 ± 112.6e	3199.3 ± 213.4d	6139.2 ± 437.6a	4842.2 ± 178.5c
Phloem area (µm2)	337.2 ± 22.5a	73.5 ± 3.6c	127.1 ± 10.9b	15.6 ± 0.97f	31.1 ± 1.28d	25.9 ± 1.01e	23.3 ± 1.78e	35.5 ± 2.37d
Pith radius (µm)	1235.6 ± 118.7a	817.7 ± 58.9b	563.3 ± 44.6d	236.2 ± 19.7f	472.4 ± 22.4e	617.8 ± 43.2c	526.9 ± 44.6d	726.8 ± 42.6c
Pith cell area (µm2)	6830.9 ± 345.7b	7695.6 ± 413.7a	6485.1 ± 550.7b	1037.6 ± 112.3d	4582.8 ± 217.8c	4150.4 ± 312.3c	4582.8 ± 288.6c	6139.2 ± 440.8b
Stem radius (µm)	2325.8 ± 125.4a	1671.6 ± 113.5c	1405.1 ± 112.6c	1005.4 ± 102.4e	1223.4 ± 106.3d	1744.3 ± 143.7b	1708 ± 155.7b	1714 ± 143.8b
Leaf anatomical parameters								
Lamina thickness (µm)	199.9 ± 11.99e	272.6 ± 13.4d	345.2 ± 26.7b	272.6 ± 14.5d	308.9 ± 28.9c	345.2 ± 29.7b	308.9 ± 27.7c	417.9 ± 32.09a
Mesophyll thickness (µm)	127.2 ± 7.8c	109.0 ± 4.3d	127.2 ± 6.4c	127.2 ± 5.5c	218.0 ± 13.6a	218.0 ± 18.9a	127.2 ± 9.8c	145.4 ± 7.7b
Midrib thickness (µm)	417.9 ± 25.6e	514.8 ± 37.8c	708.6 ± 58.9a	545.1 ± 24.4c	417.9 ± 27.7e	417.9 ±23.2e	490.6 ± 34.4d	696.5 ± 56.5b
Epidermal thickness (µm)	54.5 ± 4.3b	72.7 ± 5.5a	41.8 ± 5.8c	54.5 ± 3.9b	45.4 ± 3.2c	27.3 ± 1.26d	54.5 ± 2.46b	54.5 ± 3.5b
Vascular tissue thickness (µm)	333.1 ± 22.8d	345.2 ± 21.6d	526.9 ± 44.8a	454.3 ± 32.6c	254.4 ± 11.5e	308.9 ± 20.7d	436.1 ± 26.6c	496.6 ± 37.4b
Leaf surface anatomical parameters								
Adaxial stomatal density (mm-2)	13.3 ± 0.21e	66.7 ± 4.56a	38.0 ± 2.34c	27.7 ± 1.7d	38.3 ± 1.08c	32.7 ± 1.44c	36.3 ± 1.55c	42.0 ± 2.58b
Adaxial stomatal area (µm2)	5966.3 ± 314.3b	1902.3 ± 113.4e	7176.8 ± 514.7a	5879.8 ± 333.4b	3372.2 ± 234.5d	4064 ± 213.4c	6052.7 ± 534.7b	4842.2 ± 298.7c
Adaxial epidermal cell area (µm2)	8473.8 ± 665.7c	7782.1 ± 444.7c	11500.2 ± 789b	4842.2 ± 312.5d	10203.2 ± 645b	3804.6 ± 415.6e	12019.0a ± 655.7a	5447.5 ± 412.9d
Abaxial stomatal density (mm-2)	70.0 ± 3.56b	123.0 ± 1.23a	70.0 ± 2.89b	44.0 ± 2.3d	23.0 ± 1.12e	42.0 ± 2.11d	69.0 ± 2.44c	50.0 ± 3.33d
Abaxial stomatal area(µm2)	6398.6 ± 556.1d	2594.0 ± 112.3e	11932.5 ± 978b	7003.9 ± 555.3c	5879.8 ± 332.3d	5966.3 ± 431.4d	23259.8 ± 897a	7955 ±555.2c
Abaxial epidermal cell area (µm2)	13748.3 ± 899.4d	15045.4 ± 665.7b	14007.7 ± 833.c	10635.5 ± 617d	16688.2 ± 798a	7349.7 ± 515.1e	14699.5 ± 945c	14180.7 ± 988c

Bold black fonts indicate the maximum value, while red bold fonts the minimum values

Number of branches was high in populations at collected from Warcha Saltmine, Khabbeki and Ladam Sar (14.3, 14.3 and 10.7 respectively). Leaf density was the maximum (51) at hypersaline salt marsh (Khabbeki). Lower plant heights (4.2 m and 3.7 m) were observed in plants growing at Ladam Sar and Khabbeki populations. Despite of high leaf density (32) in the plants from Ladam Sar, the biomass allocation was the minimum (9.0 g plant^{-1}, 1.5 g plant^{-1} shoot fresh weight and dry weight, respectively). Biomass accumulation was relatively high in Warcha Saltmine population (59.0 g plant^{-1}, 9.8 g plant^{-1} shoot fresh and dry weights, respectively (Table 2).

Physiological traits

Chlorophyll pigments: High elevation sites such as mountain spring Dape Sharif, mountain peak Fort Munro and deep valley Neela Wahn exhibited higher photosynthetic capabilities as reflected by higher levels of chlorophyll *a* (2.1 mg g^{-1}, 2.0 mg g^{-1} and 2.0 mg g^{-1}, respectively), chlorophyll *b* (1.1 mg g^{-1}, 1.0 mg g^{-1} and 1.0 mg g^{-1}, respectively) and total chlorophyll (3.2 mg g^{-1}, 3.0 mg g^{-1} and 2.0. mg g^{-1}, respectively). Hypersaline desert plain Ladam Sar, low sand dunes Nawab Shah and hypersaline saltmarsh Khabbeki exhibited lower concentration of chlorophyll pigments (Table 2).

Stress enzymes: Hypersaline desert plain Ladam Sar and hypersaline saltmarsh Khabbeki exhibited higher accumulation of catalase (5.5 U mg^{-1} protein and 5.4 U mg^{-1} protein, respectively) and superoxide dismutase (0.8 U mg^{-1} protein, 0.8 U mg^{-1} protein, respectively). The enzymes activities were relatively low at deep valley Neela Wahn (catalase; 2.2 U mg^{-1} protein, SOD 0.1 U mg^{-1} protein), and mountain spring Dape Sharif (catalase; 2.5 U mg^{-1} protein, SOD 0.3 U mg^{-1} protein). Peroxidase levels were relatively high at hypersaline desert plain Ladam Sar (7.1 U mg^{-1} protein) and hypersaline salt marsh Khabbeki (6.8 U mg^{-1} protein) (Table 2).

Osmoprotectants: Hypersaline saltmarsh Khabbeki exhibited highest total soluble sugars (23.8 µg g^{-1}), total soluble proteins (1570.5 µg g^{-1}), total free amino acids (421.5 µg g^{-1}) and proline (127.7 µmol g^{-1}). At deep valley Neela Wahn and coarse sand desert Sakhi Sarwar, total soluble proteins (572.5 µg g^{-1} and 570.8 µg g^{-1}, respectively) and total soluble sugars (12.7 µg g^{-1} and 11.5 µg g^{-1}, respectively) were low. Mountain peak Fort Munro exhibited low total soluble proteins (775.5 µg g^{-1}), total soluble sugars (8.6 µg g^{-1}) and total free amino acids (182.4 µg g^{-1}). Population at mountain spring Dape Sharif exhibited low total soluble proteins (104.1 µg g^{-1}), total soluble sugars (7.1 µg g^{-1}), total free amino acids (142.1 µg g^{-1}) and proline (82.1 µmol g^{-1}) (Table 2).

Antioxidants and vitamins: Populations at hypersaline saltmarsh Khabbeki exhibited high malondialdehyde (2.2 µmol g^{-1}), maximum hydrogen peroxide (5.0 µmol g^{-1}), maximum ascorbic acid (0.2 µg g^{-1}) and maximum phenolics (2.4 µg g^{-1}). Hypersaline desert plains Ladam Sar exhibited the maximum malondialdehyde (2.4 µmol g^{-1}), high hydrogen peroxide (4.2 µmol g^{-1}), maximum ascorbic acid (0.26 µg g^{-1}) and high phenolics (2.0 µg g^{-1}). Coarse sand desert Sakhi Sarwar showed minimum malondialdehyde (1.0 µmol g^{-1}) and hydrogen peroxide (2.9 µmol g^{-1}). Mountain peak Fort Munro exhibited minimum malondialdehyde (1.2 µmol g^{-1}) and phenolics (1.4 µg g^{-1}), and low hydrogen peroxide (3.3 µmol g^{-1}). Warcha Saltmine possessed high hydrogen peroxide (4.2 µmol g^{-1}), and maximum ascorbic acid (0.23 µg g^{-1}). Mountain spring Dape Sharif exhibited minimum malondialdehyde (1.4 µmol g^{-1}) and phenolics (1.5 µg g^{-1}) (Table 2).

Anatomical traits

Stem anatomical traits: Stem epidermal thickness was maximum in populations collected from low sand dunes Nawab Shah (60.6 µm) and was relatively high at hypersaline desert plain Ladam Sar (54.5 µm) and coarse sand desert Sakhi Sarwar (54.5 µm). Stem sclerification was highest at hypersaline desert plain area Ladam Sir (sclerenchyma cell area 354.5 µm^2 and sclerenchyma thickness 133.2 µm). Stem sclerification was lowest at coarse sand desert Sakhi Sarwar (sclerenchyma cell area 5.2 µm^2; sclerenchyma thickness 54.5 µm). Sclerenchyma cell area was relatively high at deep valley Neela Wahn (233.5 µm^2), hypersaline saltmarsh Khabbeki (145.3 µm^2) and salt affected dry lands Ladam Sar (145.3 µm^2). Low sand dunes Nawab Shah and mountain spring Dape Sharif exhibited high stem cortical cell area (1297 µm^2 and 778.2 µm^2, respectively) and stem cortical thickness (218 µm and 254.4 µm, respectively). Coarse sand desert exhibited minimum stem cortical thickness (54.5 µm), whereas populations at salt affected dry land Ladam Sar exhibited minimum stem cortical cell area (5.2 µm^2) (Table 3 and Fig. 2).

Hypersaline salt marsh had maximum stem vascular bundle thickness (1066 µm), xylem thickness (999.4 µm) and broad metaxylem area (6139.2 µm^2). Deep valley Neela Wahn exhibited maximum stem metaxylem area (6485.1 µm^2), whereas coarse sand desert Sakhi Sarwar exhibited minimum metaxylem area (454 µm^2). Mountain peak Fort Munro exhibited low stem vascular bundle thickness (581.4 µm), xylem thickness (563.3 µm) and metaxylem cell area (1642.9 µm^2). Low sand dunes Nawab Shah exhibited maximum stem phloem area (337.2 µm^2) (Table 3 and Fig. 2).

Low sand dunes Nawab Shah showed highest stem radius (2325.8 µm) and pith radius (1235.6 µm) with relatively high pith cell area (6830.9 µm). Hypersaline desert plain Ladam Sar area exhibited maximum pith cell area (7695.6 µm^2) and high pith radius (817.7 µm) but relatively small stem radius (1671.6 µm). Populations at coarse sand desert Sakhi Sarwar exhibited minimum stem radius (1005.4 µm), pith radius (236.2 µm) and pith cell area (1037.6 µm^2). Populations at mountain spring exhibited small stem radius (1223.4 µm), pith radius (472.4 µm) and metaxylem area (4582.8 µm^2) (Table 3 and Fig. 2).

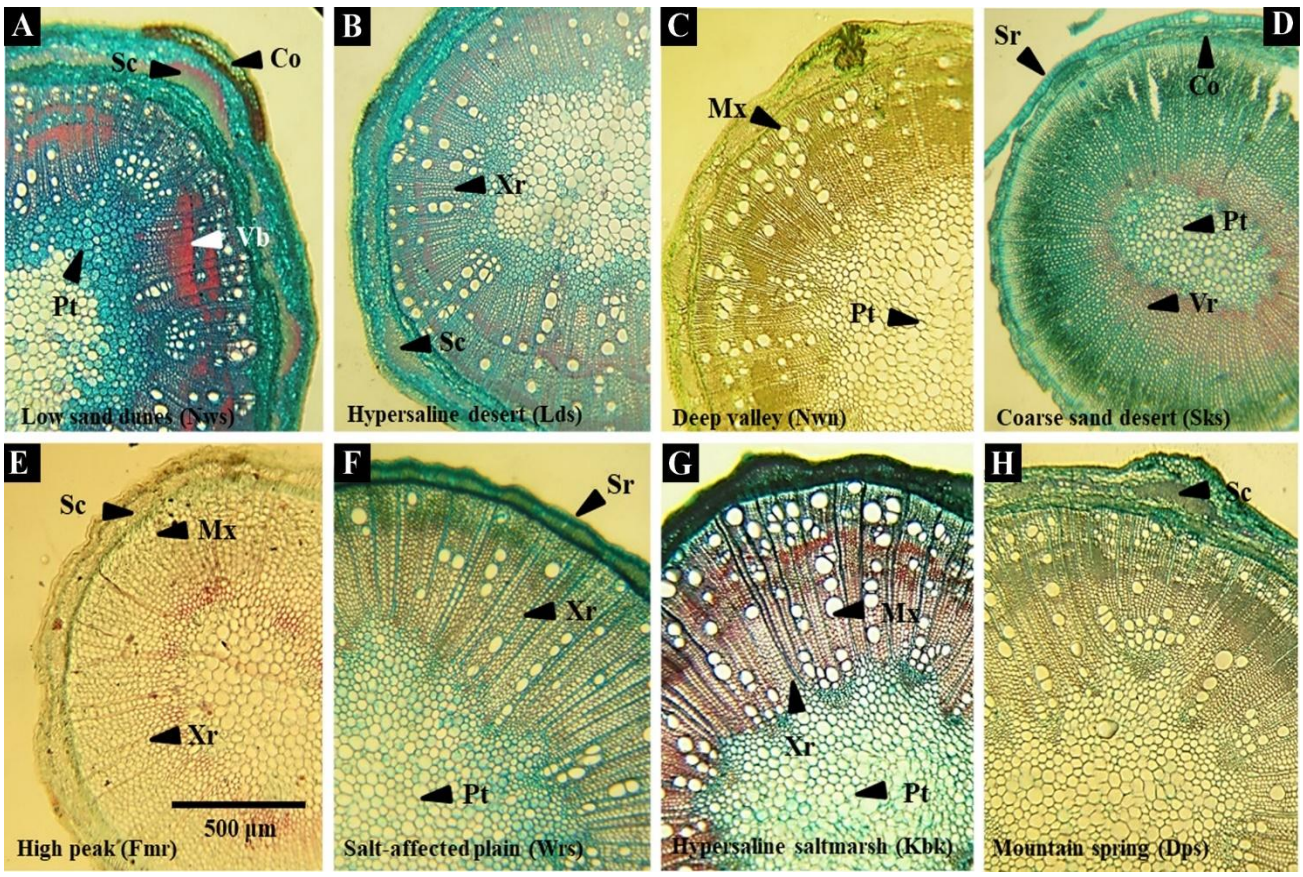

Fig. 2. Stem transverse sections of *Neltuma glandulosa* populations collected from ecologically different habitats in the Punjab. **A.** Collenchyma (Co) inside epidermis; extensive deposition of lignin in vascular tissue (Vb); Crystallization in pith region (Pt). **B.** Large sclerenchyma bundles (Sc) in the cortical region; Distinct xylary rays (Xr) between vascular bundles; **C.** Numerous broad metaxylem vessels (Mx) in xylem tissue; Enlarge pith region (Pt). **D.** Greatly reduced stem radius (Sr), cortical region (Co) and pith region (Pt); Greatly increased proportion of vascular tissue (Vr). **E.** Large sclerenchyma bundles (Sc) in the cortical region; Low lignification in the vascular region (Vr); Metaxylem vessels (Mx) small and indistinguishable from other xylem tissue. **F.** Greatly increased stem radius (Sr); Increased xylem (Xr) thickness; Increased pith region (Pt). **G.** Greatly increased number and size of metaxylem vessels; Thickest xylem region; Increased pith region. **H.** Large sclerenchyma bundles (Sc) in the cortical region.

Ionic content: Hypersaline saltmarsh Khabbeki exhibited maximum shoot K^+ (11.5 mg g^{-1}) and shoot Na^+ (42.6 mg g^{-1}). Hypersaline desert plain Ladam Sar exhibited high shoot Na^+ (41.4 mg g^{-1}) and maximum shoot Ca^{2+} (33.4 g^{-1}). Low sand dunes Nawab Shah exhibited minimum shoot K^+ (3.3 mg g^{-1}) and Na^+ (19.3 mg g^{-1}). The Warcha Saltmine exhibited high Na^+ (38.2 mg g^{-1}) and K^+ (9.6 mg g^{-1}), and minimum Ca^{2+} (8.2 mg g^{-1}). Coarse sand desert Sakhi Sarwar exhibited low shoot Na^+ (10.2 mg g^{-1}), low K^+ (5.3 mg g^{-1}) and minimum Ca^{2+} (18.9 g^{-1}) (Table 2).

Leaf anatomical traits: Populations at mountain spring Dape Sharif exhibited the maximum lamina thickness (417.9 µm), high mesophyll thickness (145.4 µm), high midrib thickness (696.5 µm), high vascular thickness (496.6 µm) and high epidermal thickness (54.5 µm) (Table 3 and Fig. 2). Populations at deep valley Neela Wahn exhibited maximum midrib thickness (708.6 µm) and vascular thickness (526.9 µm). Populations at mountain peak Fort Munro and salt affected dry lands Warcha Saltmine exhibited maximum mesophyll thickness (218.0 µm). Population at hypersaline desert plain Ladam Sar area exhibited maximum epidermal thickness (72.7 µm), small lamina thickness with the minimum mesophyll thickness (109.0 µm), small midrib with small vascular tissue. Low sand dunes Nawab Shah exhibited minimum lamina thickness (199.9 µm) and small mesophyll thickness and minimum midrib thickness (417.9 µm) with small vascular tissue.

Leaf surface anatomical traits: Population at hypersaline desert plain area Ladam Sar exhibited maximum adaxial and abaxial stomatal density (66.7 per mm^2 and 123 per mm^2, respectively) but the minimum stomatal area on both surfaces (Table 3 and Fig. 4). Abaxial epidermal cell area (15045.4 μm^2) at Ladam Sar was relatively high, in contrast to adaxial epidermal cell area (7782.1 μm^2). Populations at low sand dunes Nawab Shah exhibited minimum adaxial stomatal density (13.3 per mm^2), in contrast to high abaxial stomatal density (70 per mm^2). Stomatal area was comparatively large and epidermal cell area was relatively low on both surfaces at Nawab Shah. Populations at salt affected dry land Warcha Saltmine exhibited low stomatal densities, lower stomatal cell areas and the minimum epidermal cell areas on both adaxial and abaxial leaf surfaces. Populations at mountain peak Fort Munro exhibited minimum abaxial stomatal density (23 per mm^2) and the maximum abaxial epidermal cell area (16688.2 μm^2).

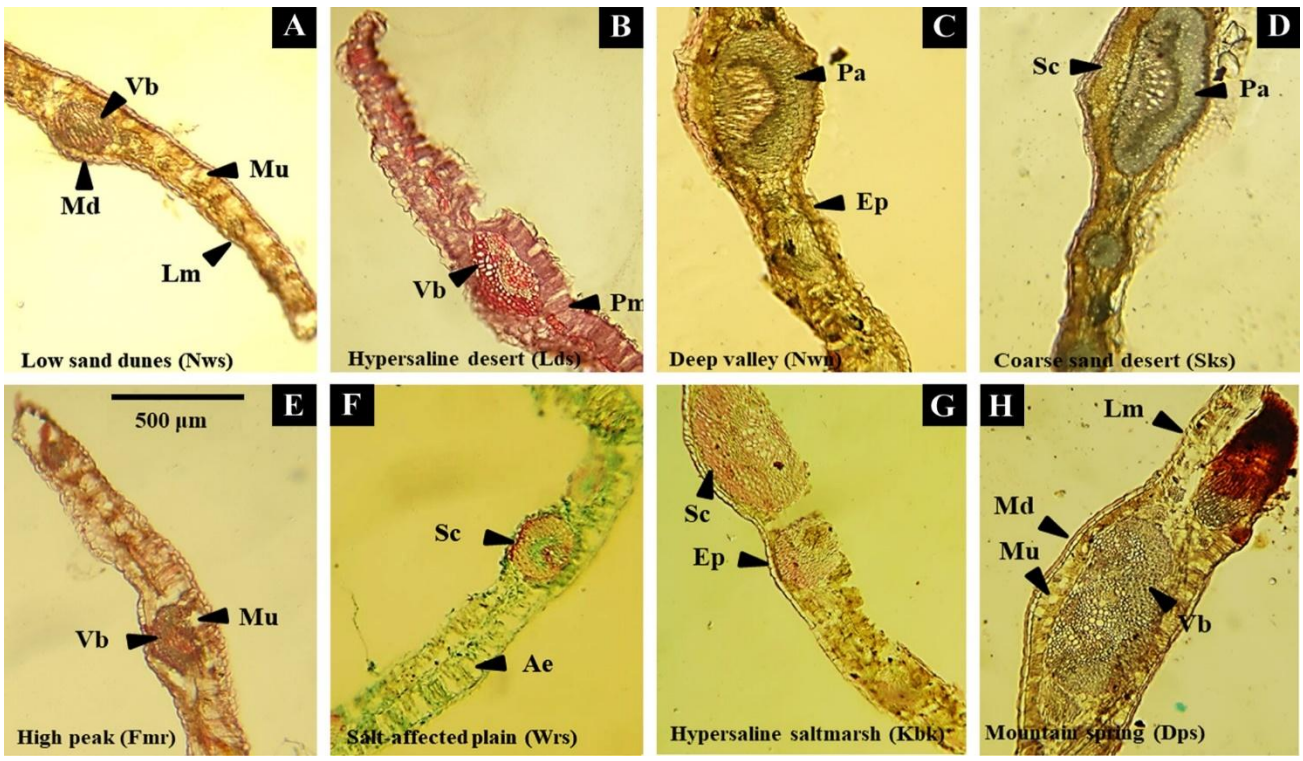

Fig. 3. Leaf transverse sections of *Neltuma glandulosa* populations collected from ecologically different habitats in the Punjab.
A. Greatly reduced midrib (Md) and lamina (Lm) thickness; Greatly reduced vascular bundle (Vb) area; Several mucilaginous cavities (Mu) in mesophyll. **B.** Extensive sclerification in vascular bundles (Vb); Enlarged palisade mesophyll (Pm). **C.** Enlarged parenchyma region; Thick epidermis on both leaf surfaces. **D.** Enlarged parenchyma (Pa) region; Extensive sclerification (Sc) outside vascular bundle. **E.** Large mucilaginous cavities (Mu) in midrib; Reduced vascular bundle (Vb) area. **F.** Large air cavities (Ae) in the palisade mesophyll. Extensive sclerification (Sc) on abaxial side outside vascular bundles. **G.** Abaxial epidermal cells (Ep) enlarge; Extensive sclerification (Sc) outside vascular bundles at abaxial side. **H.** Greatly enlarged midrib (Md) and lamina (Lm) thicknesses; Greatly enlarged vascular bundle (Vb); Numerous mucilaginous cavities in the midrib region.

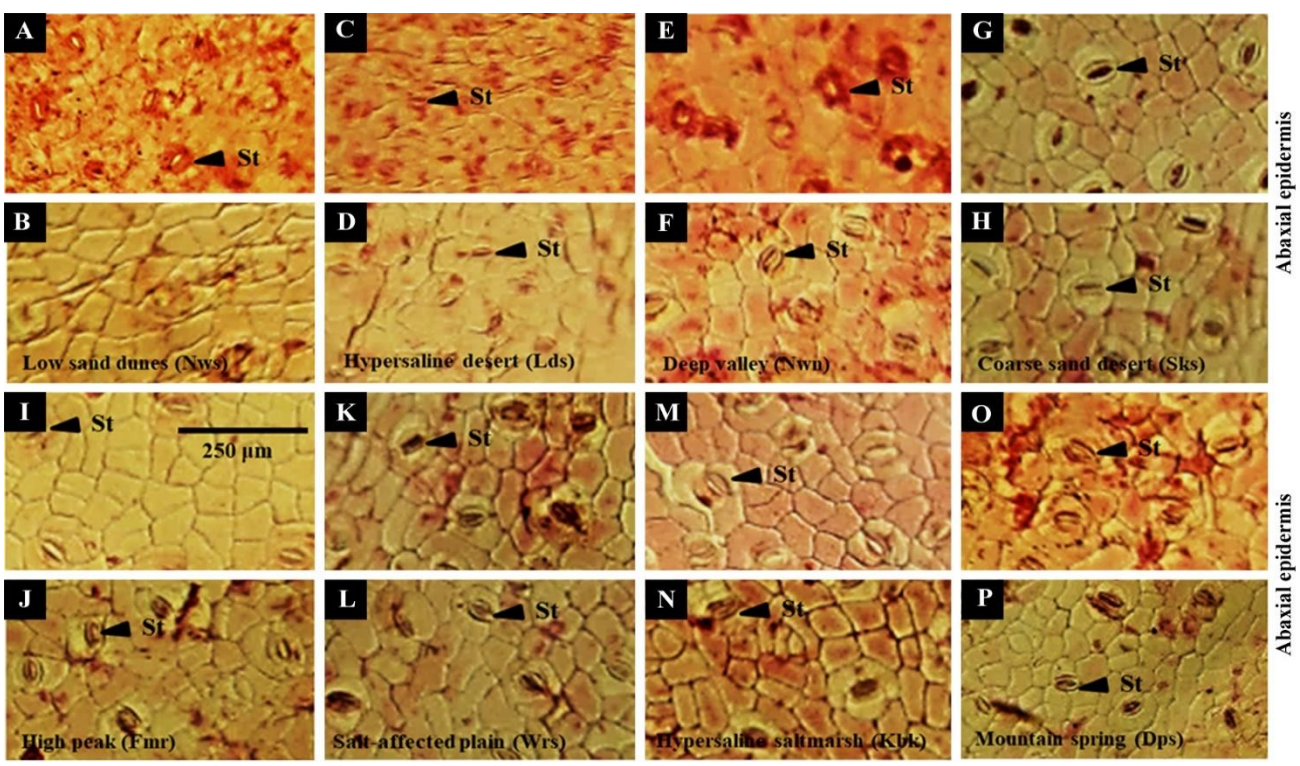

Fig. 4. Leaf surface view of *Neltuma glandulosa* populations collected from ecologically different habitats in the Punjab. St–Stomata
A. Stomata small and elliptic on abaxial surface; **B.** Stomata absent on adaxial surface. **C.** Stomatal size greatly reduced on abaxial surface; **D.** Stomata small, narrowly elliptic on adaxial surface. **E.** Stomatal density greatly reduced on abaxial surface, while size increased significantly; **F.** Stomata large, elliptic on adaxial surface. **G & H.** Stomata size and density increased on both leaf surfaces. **I.** Stomata narrowly elliptic on abaxial surface; **J.** While small and broadly elliptic on adaxial surface. **K.** Stomata numerous and round on abaxial surface; **L.** While elliptic and small on adaxial surface. **M.** Stomata elliptic on abaxial surface; **N.** While narrowly elliptic on adaxial surface. **O.** Stomata large and broadly elliptic on abaxial surface; **P.** While small and elliptic on adaxial surface.

Principal component analysis: Relationship among environmental, soil physicochemical, morphological, stem anatomical and leaf anatomical traits is presented (Fig. 5a). Soil organic matter, Ca^{2+}, NO_3^- and PO_4^{3-} were clustered with high peak Fort Munro and coarse sand desert Sakhi Sarwar. Plant height and leaf mesophyll thickness were associated with salt affected plain Warcha Saltmine, deep valley Neela Wahn, and mountain spring Dape Sharif were interconnected with environmental traits (average rainfall and elevation), morphological traits (number of branches, leaf area, and shoot fresh and dry weights), stem anatomical traits (metaxylem area) and leaf anatomical traits (lamina thickness, vascular tissue thickness, midrib thickness, mesophyll thickness, and adaxial and abaxial stomatal area). Hypersaline saltmarsh was grouped with soil traits such as saturation percentage, pH, ECe and soil Na^+, stem anatomical traits such as metaxylem area, pith cell area, stem radius, cortical cell area, sclerenchyma thickness and vascular bundle thickness, and leaf anatomical traits such as adaxial and abaxial epidermal cell area and adaxial stomatal density. Hypersaline desert Ladam Sar and low sand dunes Nawab Shah were closely associated with minimum and maximum temperature, stem anatomical traits such as pith radius, sclerenchyma cell area and phloem area, and leaf anatomical traits such as epidermal thickness and abaxial stomatal density.

Relationship among environmental, soil physicochemical, morphological and physiological traits is presented (Fig. 5b). Coarse sand desert Sakhi Sarwar was associated with soil traits such as PO_4^{3-}, NO_3^- and organic matter, which influenced chlorophyll *a*/*b* ratio. Mountain peak Fort Munro, deep valley Neela Wahn and mountain spring showed close association with peroxidase, malondialdehyde, total soluble proteins, hydrogen peroxide, shoot Na^+, ascorbic acid, superoxide dismutase, catalase and phenolics, which were linked to plant height, leaf area, and shoot fresh and dry weights. Hypersaline saltmarsh Khabbeki was related to annual rainfall, soil traits such as saturation percentage, ECe, Na^+ and K^+, and physiological traits such as proline, carotenoids, chlorophyll *a*, total chlorophyll, chlorophyll *b* and shoot K^+, which influenced number of leaves and number of branches.

Discussion

Overall structural and functional response and mechanism of adaptation of the *N. glandulosa* population to environmental heterogeneity is summarized (Table 4 and Fig. 6). Low sand dunes in the Cholistan Desert Nawab Shah were exposed to extremely hot temperature and hyperaridity, with low rainfall. Ladam Sar hypersaline Cholistan Desert faced hyperaridity, hypersalinity and extremely hot temperature. Neela Wahn deep valley in the Salt Range is situated between dry sandstone mountains and had relatively low temperature. Sakhi Sarwar coarse sand desert was subjected to hyperaridity and extremely hot temperature. Fort Munro was the highest peak in the Suleman Range, which was exposed to aridity and extremely cool temperature. Salt-affected plains at Warcha Saltmine had aridity and hypersalinity, while hypersaline saltmarsh at Khabbeki was surrounded by sandstone dry mountains and subjected to aridity, hypersalinity and relatively low temperature. Dape Sharif population was collected from the bank of mountain spring, which was exposed to relatively low temperature. Three sites were heavily salt-affected, namely Khabbeki, Ladam Sar and Warcha Saltmine, soil of the other sites were non-saline.

Plants ability to adapt in an environmental heterogeneity mainly relies on plasticity in structural and functional traits that modifies with a specific set of climatic conditions (Westerband *et al*., 2021). There is evidence that functional trait variation is significant for plant populations that are undergoing fast environmental change (Malik *et al*., 2024). Microenvironmental variability in abiotic and biotic variables, such as air temperature, and aridity, greatly influences functional features (García-Cervigón *et al*., 2021). Evidence suggests that variation in functional traits plays an important role for plant populations experiencing rapid environmental change. Functional traits are strongly driven by microenvironmental heterogeneity in abiotic and biotic factors, including irradiance, air temperature and aridity, as well as competition and herbivory.

No invasive species has been recorded in the desert ecosystem of Pakistan, buet there are few examples on global scale. The Mojave Desert has been invaded by non-native annual grasses like *Bromus* and *Schismus*, which have deteriorated habitat by increasing the frequency and intensity of fires and changing the composition of plant communities (Smith *et al*., 2023). *Bromus tectorum* is one of the most common and troublesome invaders in North American deserts, making it one of the most urgent ecological issues on the planet (Dosdall *et al*., 2024). Particularly because of recurrent fires and interannual variations in precipitation, invasive grass, *Pennisetum ciliare*, proliferate quickly into native desert habitats (Ravi *et al*., 2022).

Environmental conditions, such as mesic, xeric and saline environments greatly influence plant growth and development (Singh, 2024). More tolerant species have tremendous ability to cope with environmental heterogeneity, which might be due to huge plasticity in macro-micromorphological traits as well as functional traits (Assaeed *et al*., 2023). Growth in terms of number of branches and number of leaves per branch was the lowest in population collected from harsh hyperarid and extremely hot environments of the Cholistan low sand dunes. Restricted growth is extremely beneficial for the survival of this population (Lipiec *et al*., 2013) because it is less exposed to hot and arid climate, hence can regulate transpiration rate significantly (Sadok *et al*., 2021) and consequently lowers water loss from the plant surface (López *et al*., 2021).

In order to counteract oxidative stress caused by highly harsh surroundings, the Ladam Sar population builds up high concentrations of stress enzymes (catalase, superoxide dismutase, and peroxidase) under hypersaline, hyperarid, and extremely hot conditions (Mann *et al*., 2023). Malondialdehyde, an antioxidant, also shields this population from oxidative damage and environmental stresses (Sachdev *et al*., 2021). In addition to aiding in photosynthesis, carotenoids can also function as oxidants (Polyakov *et al*., 2023). A crucial nutrient for plants is shoot Ca^{2+} that is necessary for a number of structural functions in membranes and cell walls. In the vacuole, it acts as a counter-cation for both organic and inorganic anions, particularly competing with Na^+ in high salinity conditions (Shabbir *et al*., 2022).

Table 4. Collection sites with abiotic stressors, and mechanism of adaptation to cope abiotic stresses in Neltuma glandulosa collected from diverse habitats.

Collection sites	Stressors	Mechanism of adaptation
Nawab Shah low sand dunes	Hyperaridity, extremely hot temperature	Reduced leaves and branches per plant regulate transpiration rate. Thick epidermis controls water loss, increased cortical cell area. pith area and stem radius assist in water conservation
Ladam Sar hypersaline desert	Hyperaridity, hypersalinity, extremely hot temperature	High production of stress enzymes and antioxidants are critical for survival. Increased stem sclerification minimizes water loss and protects metabolically active tissue, and pith cell area can store more water. Thick epidermis prevents water loss through leaf surface, while increased stomatal density and decreased stomatal area regulate stomatal opening and closing more efficiently
Neela Wahn deep valley	Aridity, cool temperature	Better growth in terms of shoot fresh and dry weights. Increased metaxylem area can conduct more water and nutrients. Increased leaf thickness and stomatal may be linked to better growth.
Sakhi Sarwar coarse sand desert	Hyperaridity, hot temperature	Reduced accumulation of chlorophyll pigments, organic osmolytes and antioxidants. Reduced stem cortical and pith parenchyma can save metabolic energy, while narrow metaxylem vessels are less prone to embolism and cavitation
Fort Munro high peak	Aridity, cool temperature	High accumulation of carotenoids and thick mesophyll may increase photosynthetic capacity and large abaxial epidermal cells on abaxial prevents water loss through leaf surface.
Warcha Saltmine salt affected plain	Aridity, hypersalinity	Plants attained bushy habit due to increased number of branches. Shoot Ca2+ severely affected in this population, with a significant reduction in epidermal cell area. This will increase rate of gaseous exchange and evapotranspiration through leaf surface
Khabbeki hypersaline saltmarsh	Hypersalinity, cool temperature	The Khabbeki population adopts defensive strategies through organic osmolytes that minimize tissue damage under hypersaline conditions. In addition, survival of this population primarily depends upon high accumulation of stress enzymes and antioxidants. The K+ ion interfered with Na+ to maintain ion homeostasis in shoots. Growth was promoted in this population in terms of number of branches and number of leaves
Dape Sharif mountain spring	Hyperaridity, cool temperature	Leaf area and lamina thickness increased in this population, and this might be due to a significant increase in chlorophyll pigments (chlorophyll a and b, and carotenoids). High accumulation of glycine betaine in this population is critical for the maintenance of osmotic pressure. Moreover, thick cortical parenchyma can store more water

Steep slopes and comparatively low temperatures cause aridity, which enhanced plant growth and carotenoids content as measured by fresh and dry weights of the shoots. In plants, carotenoids provide photoprotection through non-photochemical quenching and absorb light energy for use in photosynthesis (Maslova *et al*., 2021). Carotenoids are antioxidants that can counteract dangerous free radicals and shield cells from injury (Dewanjee *et al*., 2021).

The *N. glandulosa* population of Sakhi Sarwar was gathered from a coarse-sand desert that was hot and dry and had little capacity to hold water. According to Salama *et al*., (2022) in *Alhagi graecorum*, the climate at this collection site significantly impacted the chlorophyll pigments while increasing the chlorophyll *a*/*b* ratio. This population may have limited growth and development as a result of reduced accumulation of organic osmolytes and antioxidants (Singh *et al*., 2022). Narrow metaxylem vessels are less likely to emboil and cavitate (Ren *et al*., 2023), and reduced stem cortical and pith parenchyma can save metabolic costs (Sidhu & Lynch, 2023).

Because of the steep mountain slopes, plants at Fort Munro High Peak were exposed to aridity and low temperatures. According to Pashkovskiy *et al*., (2021), a high concentration of carotenoids and thick mesophyll may boost photosynthetic capacity, and thick abaxial epidermal cells on the abaxial side stop water loss through the leaf surface (Machado *et al*., 2021). The abaxial leaf surface's low stomatal density can significantly regulate the photosynthetic rate (Wall *et al*., 2022).

In addition to being arid due to the uneven hilly terrain, the Warcha Saltmine population was gathered from hypersaline dry land. As the number of branches rose, the plants developed a bushy character. In this population, shoot Ca^{2+} was significantly impacted, as reported by Naz *et al*., 2024 in *Cressa cretica.* The area of epidermal cells was significantly reduced. Fatima *et al*., (2021) also reported similar findings in *Cymbopogon jwarancusa* collected from hyperarid and hypersaline desert. The rate of gaseous exchange and evapotranspiration through the leaf surface will rise thin epidermal layer (Momayyezi *et al*., 2022).

The Khabbeki hypersaline lake's high salinity and comparatively lower temperature encouraged the growth of branches and leaves, indicating the population's preference for salt (Asghar *et al*., 2023). Under hypersaline conditions, the Khabbeki population used organic osmolytes as defensive mechanisms to reduce tissue damage (Mehta & Vyas, 2023). Furthermore, a significant concentration of stress enzymes and antioxidants is essential for this population's survival (García-Caparrós *et al*., 2021). Plants accumulate stress enzymes, including superoxide dismutase, catalase and peroxidase to detoxify reactive oxygen species and mitigate the damaging effects of stress, enhancing their tolerance to various environmental challenges. These enzymes are part of a complex antioxidant defense system that helps plants to cope with various stress conditions, including drought, salinity, and high temperatures (Sachdev *et al*., 2021). In order to preserve ion homeostasis in shoots, the K^+ ion interacted with Na^+, as reported by Basu *et al*., (2021) in crop plants.

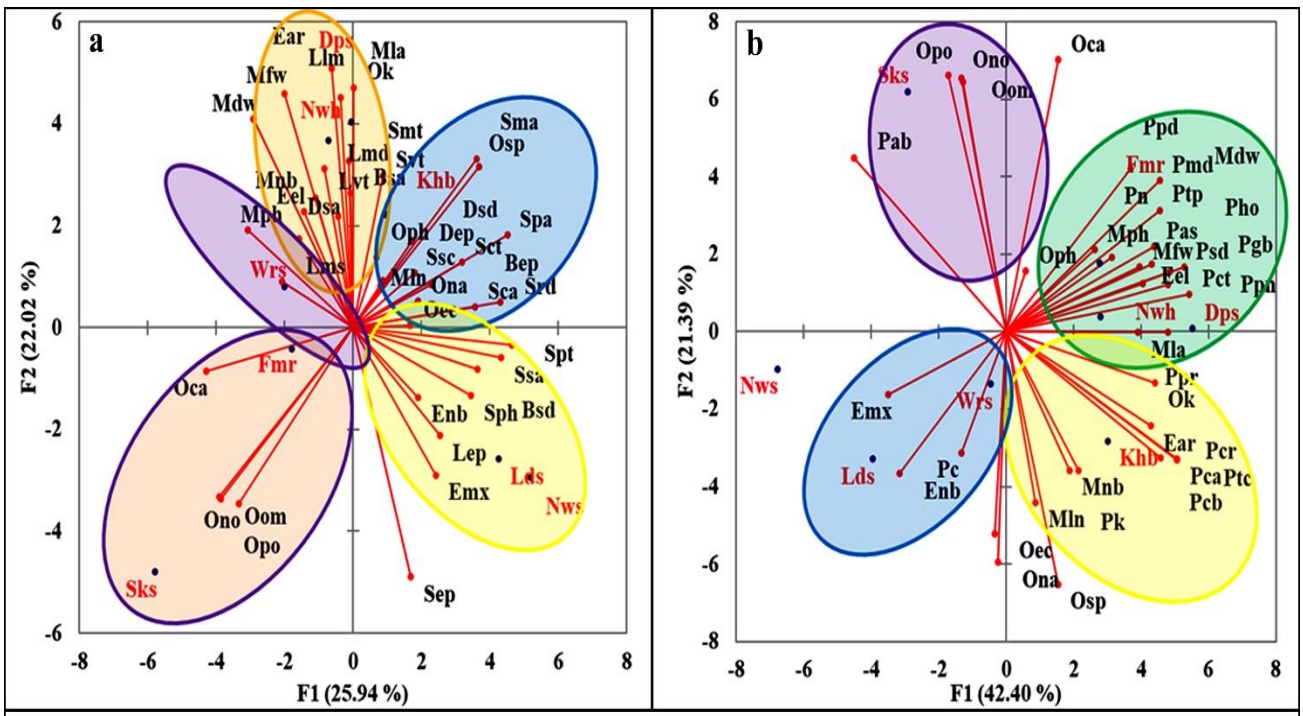

Environmental traits: Eel-Altitude, Emx - Maximum average temperature, temperature, Ear - Annual rainfall.
Soil physicochemical traits: Oec ECe, Oph - Soil pH, Oom Organic matter, Osp - Saturation percentage, Oca - Ca^{2+}, Ok - K^{+}, Ona - Na^{+}, Ono NO_3, Opo - PO_4^{3-}.
Morphological traits: Mnb - Number of branches, Mph Plant height, Mln Number of leaves per branch, LA Leaf area, Mfw Shoot fresh weight, Mdw Shoot dry weight.
Physiological traits: Ppn Phenolics, Ppr - Proline, Pgb - Glycine betaine, Pca - Chlorophyll *a*, Pcb Chlorophyll *b*, Ptc - Total chlorophyll, Pab - Chlorophyll *a*/*b* ratio, Pcr Carotenoids, Pct Catalase, Ppd Peroxidase, Psb Superoxide dismutase, Ptp - Total soluble proteins, Pmd Malondialdehyde, Pho Hydrogen peroxide, Psa Ascorbic acid, Pk - Shoot K^{+}, Pn Shoot Na^{+}, Pc - Shoot Ca^{2+}.
Stem anatomical traits: Sep - Epidermis thickness, Ssa Sclerenchyma cell area, Ssc - Sclerenchyma thickness, Sct Cortical thickness, Sca Cortical cell area, Svt Vascular bundle thickness, Smt - Xylem thickness, Sma Metaxylem area, Sph Phloem area, Spt - Pith radius, Spa - Pith cell area, Srd - Stem radius.
Leaf anatomical traits: Llm - Lamina thickness, Lms - Mesophyll thickness, Lmd - Midrib thickness, Lep - Epidermal thickness, Lvt - Vascular tissue thickness, Dsd - Adaxial stomatal density, Dsa - Adaxial stomatal area, Dep - Adaxial epidermis cell area, Bsd - Abaxial stomatal density, Bsa Abaxial stomatal area, Bep - Abaxial epidermis cell area.
Collection sites: Nwn - Neela Wahn, Dps - Dape Shrif, Kbk - Khabbeki, Wrs - Warsha Saltmine, Sks - Sakhi Sarwar, Fmr - Fort Manru, Lds - Landamsar, Nws - Nawab Shah

Fig. 5. Principal component analysis showing relationship among habitats with environmental, soil physicochemical, stem anatomical and leaf anatomical traits of *Neltuma glandulosa*.
a. Relationship among environmental, soil physicochemical, morphological, stem anatomical and leaf anatomical traits.
b. Relationship among environmental, soil physicochemical, morphological and physiological traits.
Principal Component Analysis (PCA), PC1 (F1) and PC2 (F2) represent the first and second principal components, respectively, capturing the most and second most variation in a dataset.

Despite the comparatively low average temperature, plants thrived along the side of the Dape Sharif mountain spring. Leaf area and mesophyll thickness was enhanced by adequate water availability and mild temperatures, which may have contributed to a notable rise in chlorophyll pigments (carotenoids and chlorophyll *a* and *b*), whereas enhanced cortical parenchyma allows parenchymatous cells to store more water (Ahmad *et al*., 2023).

Ecosystem dynamics are impacted by invasive species, especially in disturbed situations where human activity frequently leads to degraded land. By exploring these ideas further, we may comprehend the biological dynamics of disrupted ecosystems and create useful strategies for controlling invasive species and reestablishing the sustainability of ecosystems over the long run (Khattak *et al*., 2024). High dispersal capabilities, quick development with short generation times, and a high tolerance for a wide range of environmental circumstances are characteristics of invasive species. All together, these characteristics are linked to successional species, irrespective of their place of origin. These characteristics significantly improve a species' capacity to adjust to new environments and deal with abrupt changes in the environment, including those brought on by climate unpredictability and change. The range of invasive species will most likely shift as a result of climate change since populations of these species react to variations in temperature, moisture, and biotic interactions. It is challenging but necessary to forecast how invasive species will react in various climate change scenarios in order to

create efficient preventive, control, and restoration plans (Venette *et al*., 2021).

Sites invaded by *Neltuma* exhibited greater species variety, richness, and evenness. However, the presence of more weedy species in addition to *Neltuma* species was the cause of the increase in species richness (Kumar & Mathur, 2014). Soil pH, exchangeable Na^+, water soluble Ca^{2+} + Mg^{2+}, water soluble Na^+, and exchangeable sodium were all considerably impacted by the *Neltuma* invasion. In comparison to non-invaded lands, the invasion of *Neltuma* considerably raised the pH of the soil while decreasing the percentage of exchangeable sodium, exchangeable Na^+, and water-soluble Ca^{2+} + Mg^{2+} (Shiferaw *et al*., 2021).

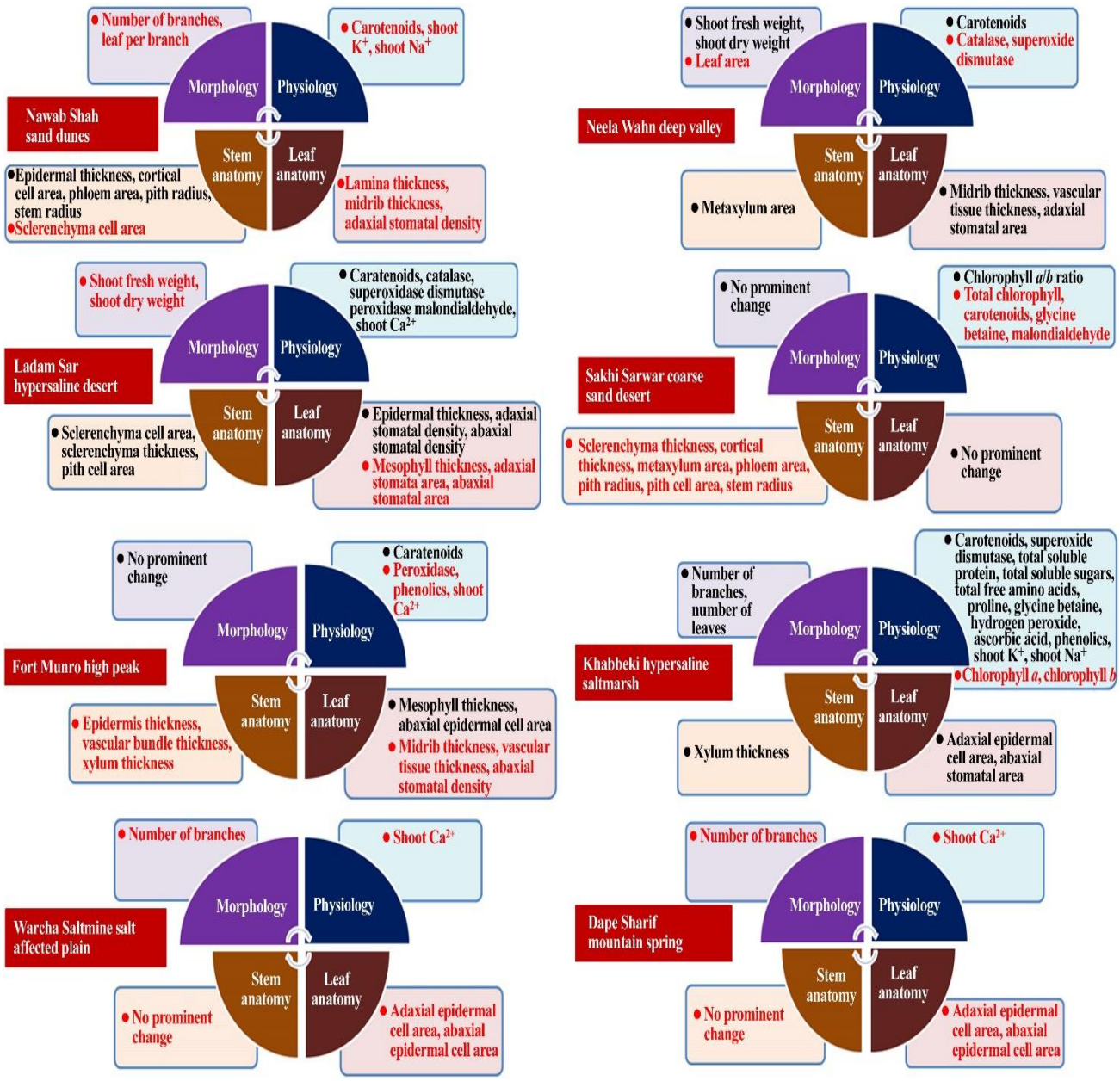

Fig. 6. Flowchart showing overall modifications in structural and functional traits *Neltuma glandulosa* collected from ecologically different habitats.
Red font colour represents the lowest value while black the highest value of morphological, anatomical and physiological traits.

Conclusions

Exceptionally high variation was recorded in macro- and micromorphological traits, chlorophyll pigments, stress enzymes, organic osmolytes, antioxidants, vitamins, ionic content, and stem and leaf anatomical traits. This reflects to the high adaptable potential of *N. glandulosa* to invade environmental heterogeneity, i.e., saline wetlands and saltmarshes, dry land salinity, high mountains, hilly tracts, coarse and fine sand deserts, and hypersaline hyperarid deserts. Plant growth and development was better in the populations collected from non-saline habitats, hot sand dune population adversely affected all growth traits. The population from haypersaline saltmarsh accumulated high concentration of organic osmolytes, stress enzymes, antioxidants and vitamins than all other populations. The hypersaline hyperarid population stored significantly high concentration of stress enzymes.

Anatomically, the sand dune desert population was better in water conversation because of thick epidermis, large parenchymatous cells, which protect water loss and stored sufficient amount of water in the stem. Stem sclerification was extraordinarily high in the hypersaline hyperarid population, supporting this population to cope with environmental adversaries. Leaf thickness and vascular tissue thickness was promoted in the populations collected from non-saline habitats. Increased stomatal density and decreased stomatal area in the population collected from hypersaline hyperarid environments assist stomatal regulation; hence play an important role in lowering transpiration loss. On the whole, invasiveness success of this species strongly relied on plasticity in structural and functional traits, which guaranteed spread of this species all over the Punjab province.

References

Abbas, A.M., A.E. Rubio-Casal, A. De Cires, B.J. Grewell and J.M. Castillo. 2019. Differential tolerance of native and invasive tree seedlings from arid African deserts to drought and shade. *S. Afr. J. Bot.*, 123:228-240. https://doi.org/10.1016/j.sajb.2019.03.018.

Ahmad, I., M. Sohail, M. Hameed, S. Fatima, M.S.A. Ahmad, F. Ahmad, A. Mehmood, S. Basharat, A. Asghar, S.M.R. Shah and K.S. Ahmad. 2023. Morpho-anatomical determinants of yield potential in *Olea europaea* L. cultivars belonging to diversified origin grown in semi-arid environments. *Plos One*, 18: e0286736. https://doi.org/10.1371/ journal.pone.0286736.

Akhter, N., M. Aqeel, M. Hameed, H.A.S. Alhaithloul, S.M. Alghanem, M.M. Shahnaz, M. Hashem, S. Alamri, N. Khalid, O.M. Al-Zoubi and M.F. Iqbal. 2021. Foliar architecture and physio-biochemical plasticity determines survival of *Typha domingensis* Pers. ecotypes in nickel and salt affected soil. *Environ. Poll*., 286: 117316. https://doi.org/10.1016/j.envpol.2021.117316.

Arnon, D. 1949. Copper enzymes in isolated chloroplasts polyphenoloxidase in *Beta vulgaris*. *Plant Physiol*., 24: 1-15. https://doi.org/10.1104/pp.24.1.1.

Asghar, N., M. Hameed and M.S.A. Ahmad. 2023. Ion homeostasis in differently adapted populations of *Suaeda vera* Forssk. ex JF Gmel. for phytoremediation of hypersaline soils. *Int. J. Phytorem*., 25: 47-65. https://doi.org/10.1080/15226514.2022.2056134.

Assaeed, A.M., B.A. Dar, A.A. Al-Doss, S.L. Al-Rowaily, I.A. Malik and A.M. Abd-ElGawad. 2023. Phenotypic plasticity strategy of *Aeluropus lagopoides* grass in response to heterogenous saline habitats. *Biology*, 12(4): 553. https://doi.org/10.3390/biology12040553

Avanesyan, A. and W.O. Lamp. 2021. Response of five *Miscanthus sinensis* cultivars to grasshopper herbivory: Implications for monitoring of invasive grasses in protected areas. *Plants*, 11(1): 53. https://doi.org/10.3390/ plants11010053.

Avanesyan, A., C. McPherson and W.O. Lamp. 2022. Analysis of plant trait data of host plants of *Lycorma delicatula* in the US suggests evidence for ecological fitting. *Forests*, 13(12): 2017. https://doi.org/10.3390/f13122017.

Basu, S., A. Kumar, I. Benazir and G. Kumar. 2021. Reassessing the role of ion homeostasis for improving salinity tolerance in crop plants. *Physiol. Plant.*, 171(4): 502-519. https://doi.org/10.1111/ppl.13112.

Bates, L., R.P. Waldren and I.D. Teare. 1973. Rapid determination of free proline for water-stress studies. *Plant Soil*, 39: 205-207. https://doi.org/10.1007/BF00018060.

Belnap, J.Y.E., J.A. Ludwig, B.P. Wilcox, J.L. Betancourt, W.R.J. Dean, B.D. Hoffmann and S.J. Milton. 2012. Introduced and invasive species in novel rangeland ecosystems: friends or foes? *Rangel. Ecol. Manag*., 65: 569-578. https://doi.org/10.2111/REM-D-11-00157.1

Bibi, S., A. Bibi, M.A. Al-Ghouti and M.H. Abu-Dieyeh. 2023. Allelopathic effects of the invasive *Prosopis juliflora* (Sw.) DC. on native plants: perspectives toward agrosystems. *Agronomy*, 13(2): 590. https://doi.org/10.3390/ agronomy13020590.

Bradford, M.M. 1976. A rapid and sensitive method for the quantification of microgram quantities of protein utilizing the principle of protein-dye binding. *Anal. Biochem*., 72: 248-254. https://doi.org/10.1016/0003-2697(76)90527-3.

Carmak, I. and J.H. Horst. 1991. Effects of aluminium on lipid peroxidation, superoxide dismutase, catalase, and peroxidase activities in root tips of soybean (*Glycine max*). *Physiol. Plant*., 83: 463-468. https://doi.org/10.1111/j.1399-3054.1991.tb00121.x.

Chance, B. and A.C. Maehly. 1955. Assay of catalases and peroxidases. *Methods Enzymol*., 2: 764-775. http:// dx.doi.org/10.1016/S0076-6879(55)02300-8

Chaturvedi, S., S. Tewari, V.K. Sah, S.K. Lavania and V.C. Dhyani. 2016. Improvement of fragile ecosystems through agroforestry. In: (Eds.): Tewari, S., V.K. Sahand and S.K. Lavania. Holistic Development of Agroforestry. Narendra Publishing House, Dehli, pp: 71-83.

Davies, K.M., M. Landi, J.W. van Klink, K.E. Schwinn, D.A. Brummell, N.W. Albert, D. Chagné, R. Jibran, S. Kulshrestha, Y. Zhou and J.L. Bowman. 2022. Evolution and function of red pigmentation in land plants. *Ann. Bot*., 130(5): 613-636. https://doi.org/10.1093/aob/mcac109.

Dawkins, K., J. Mendonca, O. Sutherland and N. Esiobu. 2022. A systematic review of terrestrial plant invasion mechanisms mediated by microbes and restoration implications. *Am. J. Plant Sci*., 13: 205-222. https://doi.org/10.4236/ ajps.2022.132013.

Deák, B., B. Kovács, Z. Rádai, I. Apostolova, A. Kelemen, R. Kiss, K. Lukács, S. Palpurina, D. Sopotlieva, F. Báthori and O. Valkó. 2021. Linking environmental heterogeneity and plant diversity: The ecological role of small natural features in homogeneous landscapes. *Sci. Total Environ.*, 763: 144199. https://doi.org/10.1016/j.scitotenv.2020.144199.

Dewanjee, S., N. Bhattacharjee, P. Chakraborty and S. Bhattacharjee. 2021. Carotenoids as antioxidants. In: (Eds.): Zia-ul-Haq, M., S. Dewanjee & M. Riaz. Carotenoids: structure and function in the human body. Springer Cham, Switzerland, pp: 447-473. https://doi.org/10.1007/978-3-030-46459-2.

Divisek, J., M. Chytry, B. Beckage, N.J. Gotelli, Z. Lososova, P. Pysek, D.M. Richardson and J. Molofsky. 2018. Similarity of introduced plant species to native ones facilitates naturalization but differences enhance invasion success. *Nat. Commun.*, 9: 1-10. https://doi.org/ 10.1038/s41467-018-06995-4.

Dosdall, J.D., R. Stanton, N. Kendall and S.B.S. Clair. 2024. Genotypic variation in cheatgrass germination strategies in contrasting climate conditions of the Great Basin and Mojave Deserts. *W. N. Am. Nat*., 84(1): 28-34. https://doi.org/10.3398/064.084.0103

Ellsworth, S.W., P.G. Crandall, J.M. Lingbeck and C.A. O'Bryan. 2018. Perspective on the control of invasive mesquite trees and possible alternative uses. *IForest Biogeosci. For*. 11: 577. https://doi.org/10.3832/ifor2456-011.

Falk, D.A., P.J. van Mantgem, J.E. Keeley, R.M. Gregg, C.H. Guiterman, A.J. Tepley, D.J. Young and L.A. Marshall. 2022. Mechanisms of forest resilience. *For. Ecol. Manag.*, 512: 120129. https://doi.org/10.1016/j.foreco.2022.120129.

Fatima, S., M. Hameed, N. Naz, S.M.R. Shah, M. Naseer, M.S.A. Ahmad, M. Ashraf, F. Ahmad, S. Khalil and I. Ahmad. 2021. Survival strategies in khavi grass [*Cymbopogon jwarancusa* (Jones) Schult.] colonizing hot hypersaline and arid environments. *Water Air Soil Pollut*., 232: 82. https://doi.org/10.1007/s11270-021-05050-1.

Funk, J.L., I.M. Parker, V. Matzek, S.L. Flory, E.T. Aschehoug, C.M. D'Antonio, W. Dawson, D.M. Thomson and J. Valliere. 2020. Keys to enhancing the value of invasion ecology research for management. *Biol. Invasions*, 22: 2431-2445. https://doi.org/10.1007/s10530-020-02267-9.

García-Caparrós, P., L. De Filippis, A. Gul, M. Hasanuzzaman, M. Ozturk, V. Altay and M.T. Lao. 2021. Oxidative stress and antioxidant metabolism under adverse environmental conditions: a review. *Bot. Rev.*, 87: 421-466. https://doi.org/10.1007/s12229-020-09231-1.

García-Cervigón, A.I., M.A. García-López, N. Pistón, F.I. Pugnaire and J.M. Olano. 2021. Co-ordination between xylem anatomy, plant architecture and leaf functional traits in response to abiotic and biotic drivers in a nurse cushion plant. *Ann. Bot.*, 127(7): 919-929. https://doi.org/10.1093/aob/mcab036.

Giannopolitis, C.N. and S.K. Ries. 1977. Superoxide dismutases: I. Occurrence in higher plants. *Plant Physiol.*, 59(2): 309-314. https://doi.org/10.1104/pp.59.2.309.

Gul, Z., Z.H. Tang, M. Arif and Z. Ye. 2022. An insight into abiotic stress and influx tolerance mechanisms in plants to cope in saline environments. *Biology*, 11(4): 597. https://doi.org/10.3390/biology11040597.

Hui, C. and D.M. Richardson. 2017. Invasion dynamics. Oxford University Press, GB. https://doi.org/10.1093/acprof:oso/9780198745334.001.0001.

Ibanez, I., G. Liu, L. Petri, S. Schaffer-Morrison and S. Schueller. 2021. Assessing vulnerability and resistance to plant invasions: a native community perspective. *Invasive Plant Sci. Manag*. 14: 64-74. https://doi.org/10.1017/inp.2021.15.

Julkenen-Titto, R. 1985. Phenolic constituents in the leaves of northern willows: methods for the analysis of certain phenolics. *J. Agric. Food Chem.*, 33: 213-217. https://doi.org/10.1021/jf00062a013.

Khattak, W.A., J. Sun, R. Hameed, F. Zaman, A. Abbas, K.A. Khan, N. Elboughdiri, R. Akbar, F. He, M.W. Ullah and A. Al-Andal. 2024. Unveiling the resistance of native weed communities: insights for managing invasive weed species in disturbed environments. *Biol. Rev*., 99(3): 753-777. https://doi.org/10.1111/brv.13043

Kull, C.A., C. Kueffer, D.M. Richardson, A.S. Vaz, J.R. Vicente and J.P. Honrado. 2018. Using the "regime shift" concept in addressing social-ecological change. *Geogr. Res*., 56: 26-41. https://doi.org/10.1111/1745-5871.12267.

Kumar, P., A.K. Mishra, S.K. Chaudhari., R. Singh, S.B. Pandey, R.K. Yadav and D.K. Sharma. 2021. Different *Prosopis* species influence sodic soil ecology by favouring carbon build-up and reclamation in North-West India. *Trop. Ecol*., 62: 71-81. https://doi.org/10.1007/s42965-020-00126-1.

Kumar, S. and M. Mathur. 2014. Impact of invasion by *Prosopis juliflora* on plant communities in arid grazing lands. *Trop. Ecol*., 55(1): 33-46.

Le Houérou, H.N. 2012. Salt-tolerant plants for the arid regions of the Mediterranean. In: (Eds.): Lieth, H. & A.A. Al Masoom. Towards the rational use of high salinity tolerant plants. Tasks for vegetation Science, vol 27. Springer, Dordrecht, pp: 27-40. https://doi.org/10.1007/978-94-011-1858-3_42.

Lipiec, J., C. Doussan, A. Nosalewicz and K. Kondracka. 2013. Effect of drought and heat stresses on plant growth and yield: A review. *Int. Agrophys*., 27(4): 463-477. https://doi.org/10.2478/intag-2013-0017.

López, R., F.J. Cano, N.K. Martin-StPaul, H. Cochard and B. Choat. 2021. Coordination of stem and leaf traits define different strategies to regulate water loss and tolerance ranges to aridity. *New Phytol.*, 230(2): 497-509. https://doi.org/10.1111/nph.17185.

Machado, R., L. Loram-Lourenço, F.S. Farnese, R.D.F.B. Alves, L.F. de Sousa, F.G. Silva, S.C.V. Filho, J.M. Torres-Ruiz, H. Cochard and P.E. Menezes-Silva. 2021. Where do leaf water leaks come from? Trade-offs underlying the variability in minimum conductance across tropical savanna species with contrasting growth strategies. *New Phytol.*, 229(3): 1415-1430. https://doi.org/10.1111/nph.16941.

Malik, A., K. Kumar, G. Kumari, N. Kumar and H. Singh. 2024. Application of functional traits in modelling productivity and resilience under climate change. In: (Eds.): Kumar, N. & H. Singh. Plant Functional Traits for Improving Productivity. Springer, Singapore, pp: 77-96. https://doi.org/10.1007/978-981-97-1510-7_5.

Mann, A., C. Lata, N. Kumar, A. Kumar, A. Kumar and P. Sheoran. 2023. Halophytes as new model plant species for salt tolerance strategies. *Front. Plant Sci.*, 14: 1137211. https://doi.org/10.3389/fpls.2023.1137211.

Maslova, T.G., E.F. Markovskaya and N.N. Slemnev. 2021. Functions of carotenoids in leaves of higher plants. *Biol. Bull. Rev.*, 11: pp. 476-487. https://doi.org/ 10.1134/S2079086421050078.

Mehta, D. and S. Vyas. 2023. Comparative bio-accumulation of osmoprotectants in saline stress tolerating plants: A review. *Plant Stress*, 9: 100177. https://doi.org/10.1016/j.stress.2023.100177.

Mengistu, D.A., D.A. Bekele, A.G. Gela, D.T. Meshesha and M.M. Getahun. 2023. Woody species diversity and regeneration status of Sub-Alpine forest of Mount Adama exclosure site, Northwestern highlands of Ethiopia. *Heliyon*, 9(6): e16473. https://doi.org/10.1016/ j.heliyon.2023.e16473.

Momayyezi, M., A.M. Borsuk, C.R. Brodersen, M.E. Gilbert, G. Théroux-Rancourt, D.A. Kluepfel and A.J. McElrone. 2022. Desiccation of the leaf mesophyll and its implications for CO_2 diffusion and light processing. *Plant Cell Environ*., 45(5): 1362-1381. https://doi.org/10.1111/pce.14287.

Moore, J.W. and D.E. Schindler. 2022. Getting ahead of climate change for ecological adaptation and resilience. *Science*, 376(6600): 1421-1426. https://doi.org/10.1126/science.abo3608.

Mukerjee, S.P. and M.A. Choudhuri. 1983. Implications of water stress-induced changes in the levels of endogenous ascorbic acid and hydrogen peroxide in *Vigna* seedlings. *Physiol. Plant*., 58: 166-170. https://doi.org/10.1111/j.1399-3054.1983.tb04162.x.

Naz, N., A. Asghar, S. Basharat, S. Fatima, M. Hameed, M.S.A. Ahmad, F. Ahmad, S.M.R. Shah and M. Ashraf. 2024. Phytoremediation through microstructural and functional alterations in alkali weed (*Cressa cretica* L.) in the hyperarid saline desert. *Int. J. Phytorem*., 26(6): 913-927. https://doi.org/10.1080/15226514.2023.2282044.

Osawa, T. 2020. Establishing strategic management plan for alien invasive plants in Ogasawara Islands. *Glob. Environ. Res*., 23: 21-28.

Pashkovskiy, P., V. Kreslavski, A. Khudyakova, A. Ashikhmin, M. Bolshakov, A. Kozhevnikova, A. Kosobryukhov, V.V. Kuznetsov and S.I. Allakhverdiev. 2021. Effect of high-intensity light on the photosynthetic activity, pigment content and expression of light-dependent genes of photomorphogenetic *Solanum lycopersicum* hp mutants. *Plant Physiol. Biochem*., 167: 91-100. https://doi.org/10.1016/j.plaphy.2021.07.033.

Pazzaglia, J., T.B. Reusch, A. Terlizzi, L. Marín-Guirao and G. Procaccini. 2021. Phenotypic plasticity under rapid global changes: The intrinsic force for future seagrasses survival. *Evol. Appl*., 14: 1181-1201. https://doi.org/ 10.1111/ eva.13212.

Polyakov, N.E., A.L. Focsan, Y. Gao and L.D. Kispert. 2023. The endless world of carotenoids–structural, chemical and biological aspects of some rare carotenoids. *Int. J. Mol. Sci*., 24(12): 9885. https://doi.org/10.3390/ijms24129885.

Rashid, M., S.H. Abbas and A. Rehman. 2014. The status of highly alien invasive plants in Pakistan and their impact on the ecosystem: a review. *Innov. J. Agric. Sci*., 2: 1-4.

Ravi, S., D.J. Law, J.S. Caplan, G.A. Barron-Gafford, K.M. Dontsova, J.F. Espeleta, J.C. Villegas, G.S. Okin, D.D. Breshears and T.E. Huxman. 2022. Biological invasions and climate change amplify each other's effects on dryland degradation. *Global Change Biol*., 28(1): 285-295. https://doi.org/10.1111/gcb.15919

Ren, Y., Y. Zhang, S. Guo, B. Wang, S. Wang and W. Gao. 2023. Pipe cavitation parameters reveal bubble embolism dynamics in maize xylem vessels across water potential gradients. *Agriculture*, 13(10): 1867. https://doi.org/ 10.3390/agriculture13101867.

Sachdev, S., S.A. Ansari, M.I. Ansari, M. Fujita and M. Hasanuzzaman. 2021. Abiotic stress and reactive oxygen species: Generation, signaling, and defense mechanisms. *Antioxidants*, 10(2): 277. https://doi.org/10.3390/ antiox10020277.

Sadok, W., J.R. Lopez and K.P. Smith. 2021. Transpiration increases under high-temperature stress: Potential mechanisms, trade-offs and prospects for crop resilience in a warming world. *Plant Cell Environ*., 44(7): 2102-2116. https://doi.org/10.1111/pce.13970.

Salama, F.M., M.M. Abd El-Ghani, A.E. Gaafar, D.M. Hasanin and D.A. Abd El-Wahab. 2022. Adaptive eco-physiological mechanisms of *Alhagi graecorum* in response to severe aridity in the Western Desert of Egypt. *Plant Biosys*., 156(2): 528-537. https://doi.org/10.1080/11263504.2021.1887957.

Shabbir, R., T. Javed, S. Hussain, S. Ahmar, M. Naz, H. Zafar, S. Pandey, J. Chauhan, M.H. Siddiqui and C. Pinghua. 2022. Calcium homeostasis and potential roles in combatting environmental stresses in plants. *S. Afr. J. Bot*., 148: 683-693. https://doi.org/10.1016/j.sajb.2022.05.038.

Shackleton, R.T., D.C. Le-Maitre, B.W. Van-Wilgen and D.M. Richardson. 2015. The impact of invasive alien *Prosopis* species (mesquite) on native plants in different environments in South Africa. S. *Afr. J. Bot*., 97: 25-31. https://doi.org/10.1016/j.sajb.2014.12.008.

Shackleton, R.T., D.C. Le-Maitre, N.M. Pasiecznik and D.M. Richardson. 2014. *Prosopis*: a global assessment of the biogeography, benefits, impacts and management of one of the world's worst woody invasive plant taxa. *AoB Plants*, 6: plu027. https://doi.org/10.1093/aobpla/plu027.

Shackleton, R.T., D.M. Richardson, C.M. Shackleton, B. Bennett, S.L. Crowley, K. Dehnen-Schmutz, R.A. Estevez, A. Fischer, C. Kueffer, C.A. Kull and E. Marchante. 2019. Explaining people's perceptions of invasive alien species: A conceptual framework. *J. Environ. Manag*., 229: 10-26. https://doi.org/10.1016/j.jenvman.2018.04.045.

Sharma, S., K. Arunachalam and A. Arunachalam. 2022. Morphology and physiology of *Perilla frutescens* (Linn.) Britt in relation to micro-climate and edaphic characteristics. *Trop. Ecol*., 26: 1-12. https://doi.org/10.1007/s42965-021-00195-w.

Shiferaw, W., S. Demissew, T. Bekele, E. Aynekulu and W. Pitroff. 2021. Invasion of *Prosopis juliflora* and its effects on soil physicochemical properties in Afar region, Northeast Ethiopia. *Int. Soil Water Conserv. Res*., 9(4): 631-638.

Sidhu, J.S. and J.P. Lynch. 2023. Cortical cell size regulates root metabolic cost. *Plant J.*, 118(5): 1343-1357. https://doi.org/ 10.1111/tpj.16672.

Singh, P., K.K. Choudhary, N. Chaudhary, S. Gupta, M. Sahu, B. Tejaswini and S. Sarkar. 2022. Salt stress resilience in plants mediated through osmolyte accumulation and its crosstalk mechanism with phytohormones. *Front. Plant Sci.*, 13: 1006617. https://doi.org/10.3389/fpls.2022.1006617.

Singh, V. 2024. Community Ecology. In: (Ed.): Singh, V. Textbook of Environment and Ecology. Springer, Singapore. https://doi.org/10.1007/978-981-99-8846-4_4

Smith, T.C., T.B. Bishop, M.C. Duniway, M.L. Villarreal, A.C. Knight, S.M. Munson, E.K. Waller, R. Jensen and R.A. Gill. 2023. Biophysical factors control invasive annual grass hot spots in the Mojave Desert. *Biol. Invas*., 25(12): 3839-3858. https://doi.org/10.1007/s10530-023-03142-z

Soper, F.M., T.W. Boutton and J.P. Sparks. 2015. Investigating patterns of symbiotic nitrogen fixation during vegetation change from grassland to woodland using fine scale δ15 N measurements. *Plant Cell Environ*., 38: 89-100. https://doi.org/10.1111/pce.12373.

Tabassum, I. 2015. Dynamics of natural vegetation cover, its human and environmental dimensions in Karak, Khyber Pakhtunkhwa, Pakistan. *J. Humanities Soc. Sci.*, 23: 51-64.

van Wilgen, B.W., T.E. Linders and K. Bekele. 2024. The impact of invading *Prosopis* species on biodiversity and ecosystem services. In: The Ecology and Management of Invasive Prosopis Trees in Eastern Africa (Eds.): Schaffner, U., K. Bekele, A. Ehrensperger and B.W. van Wilgen. CABI Digital Liberary, pp: 75-93. https://doi.org/10.1079/ 9781800623644.0005.

Velikova, V., I. Yordanov and A.J.P.S. Edreva. 2000. Oxidative stress and some antioxidant systems in acid rain-treated bean plants: protective role of exogenous polyamines. *Plant Sci.*, 151(1): 59-66. https://doi.org/10.1016/S0168-9452(99)00197-1.

Venette, R.C., D.R. Gordon, J. Juzwik, F.H. Koch, A.M. Liebhold, R.K. Peterson, S.E. Sing and D. Yemshanov. 2021. Early intervention strategies for invasive species management: Connections between risk assessment, prevention efforts, eradication, and other rapid responses. Invasive species in forests and rangelands of the United States: A comprehensive science synthesis for the United States Forest Sector, pp. 111-131.

Wall, S., S. Vialet-Chabrand, P. Davey, J. Van Rie, A. Galle, J. Cockram and T. Lawson. 2022. Stomata on the abaxial and adaxial leaf surfaces contribute differently to leaf gas exchange and photosynthesis in wheat. *New Phytol*., 235(5): 1743-1756. https://doi.org/10.1111/nph.18257.

Westerband, A.C., J.L. Funk and K.E. Barton. 2021. Intraspecific trait variation in plants: a renewed focus on its role in ecological processes. *Ann. Bot*., 127(4): 397-410. https://doi.org/10.1093/aob/mcab011.

Wolf, B. 1982. An improved universal extracting solution and its use for diagnosing soil fertility. Commun. *Soil Sci. Plant Anal*., 13(12): 1005-1033. https://doi.org/10.1080/ 00103628209367331.